INL/EXT-08-14627

Microstructural Characterization of Irradiated U-7 Wt% Mo Dispersion Fuels With Al Alloy Matrices that Contain Si

Dennis D. Keiser, Jr.
Adam B. Robinson
Jan-Fong Jue
Daniel M. Wachs

August 2008

The INL is a U.S. Department of Energy National Laboratory
operated by Battelle Energy Alliance

Idaho National Laboratory

INL/EXT-08-14627

Microstructural Characterization of Irradiated U-7 Wt% Mo Dispersion Fuels With Al Alloy Matrices that Contain Si

Dennis D. Keiser, Jr.
Adam B. Robinson
Jan-Fong Jue
Daniel M. Wachs

August 2008

Idaho National Laboratory
Nuclear Fuels and Materials Division
Idaho Falls, Idaho 83415

http://www.inl.gov

Prepared for the
U.S. Department of Energy
Office of Nuclear Energy
Under DOE Idaho Operations Office
Contract DE-AC07-05ID14517

ABSTRACT

U-7Mo alloy dispersion fuels with aluminum (Al) alloy matrices that contain silicon (Si) were irradiated in the Idaho National Laboratory (INL)'s Advanced Test Reactor (ATR) and then destructively examined using optical metallography and scanning electron microscopy to characterize the developed microstructures. Results were compared to the microstructures of as-fabricated dispersion fuel to determine what changes had occurred during irradiation. It was found that having Si in the matrix resulted in the formation of Si-rich fuel/matrix interaction layers around the fuel particles during the fuel element fabrication process. During irradiation, these interaction layers changed very little in thickness and in composition in many areas of a fuel plate that contained the most Si. However, in some rarely observed areas that were exposed to very aggressive irradiation conditions, the interaction layers grew in thickness and changed in composition to become Si-deficient. For a fuel plate with relatively low amounts of Si, only Si-deficient layers were observed. The overall irradiation performance to very high burnups was excellent for the fuel with the most Si in the Al alloy matrix.

ACKNOWLEDGMENTS

This work was supported by the U.S. Department of Energy, Office of Nuclear Materials Threat Reduction (NA-212), and National Nuclear Security Administration, under DOE-NE Idaho Operations Office Contract DE-AC07-05ID14517. The INL HFEF staff are thankfully acknowledged for their contributions in performing PIE and generating punchings used for conducting the SEM analysis. Dawn Janney is acknowledged for her work in the Electron Microscopy Laboratory assisting with preparation and SEM analysis of the punchings. Pavel Medvedev is acknowledged for helping with the irradiation condition calculations. Tom Weincek is acknowledged for his efforts in fabricating the dispersion fuels for the RERTR-6 experiment at ANL. INL staff are also acknowledged for the fabrication of the RERTR-7 experiment. Finally, acknowledgment is given to the ATR staff for their assistance in performing the irradiation experiments.

CONTENTS

FIGURES

TABLES

ACRONYMS

ANL	Argonne National Laboratory
ATR	Advanced Test Reactor
BOL	Beginning of Life
DOE	Department of Energy
EDS	Energy-Dispersive Spectrometer
EFPD	Effective Full-Power Days
EPMA	Electron Probe Microanalysis
HFEF	Hot Fuel Examination Facility
KAERI	Korean Atomic Energy Research Institute
LEU	Low-Enriched Uranium
PFZ	Precipitate-Free Zone
PIE	Post-Irradiation Examination
RED	Radiation Enhanced Diffusion
RERTR	Reduced Enrichment for Research and Test Reactors
SEM	Scanning Electron Microscopy
TTT	Time Temperature Transformation
WDS	Wavelength-Dispersive Spectrometer

Microstructural Characterization of Irradiated U-7 Wt% Mo Dispersion Fuels With Al Alloy Matrices that Contain Si

1. INTRODUCTION

The Reduced Enrichment for Research and Test Reactors (RERTR) program is developing low-enriched uranium (LEU) U-Mo fuels to replace highly enriched uranium fuels in research and test reactors.[1] As part of this development, a variety of irradiation experiments have been conducted in Idaho National Laboratory (INL)'s Advanced Test Reactor (ATR), with the recent focus being on the performance of U-Mo alloy fuels.[2] Initial irradiation testing of U-Mo dispersion fuels with pure Al as the matrix indicated that porosity can develop at high burnups, which may result in pillowing and eventual failure of fuel plates.[3] The formation of this porosity has been linked to the formation of a reaction product that results from interdiffusion between the U-Mo fuel and the Al matrix that does not exhibit good irradiation performance. Si additions to the matrix of a dispersion fuel may constitute a possible solution to this pillowing problem, since it may result in the stabilization of a UAl3-type of phase that exhibits better irradiation performance.[4] Diffusion studies have shown that the presence of Si does result in a change in the types of phases that will form when U-Mo fuels interact with the Al alloy cladding.[5,6,7] With respect to the irradiation performance of interaction phases that contain Si, it has been demonstrated that U3Si2 dispersion fuels, which form a U(Al,Si)3 interaction phase around the fuel particles due to interactions with the Al matrix, perform well under irradiation.[8]

To test the effects of adding Si to the matrix of U-Mo dispersion fuels, Si-containing fuel plates have been irradiated as part of the RERTR-6 and RERTR-7 irradiation experiments using the ATR. Some of these Si-containing fuel plates employed 4043 Al alloy and Al-0.2 wt% Si as the matrices. The 4043 Al alloy contains almost 5.0 wt% Si, which was the highest concentration of added Si that was tested. The lowest Si content tested was an alloy with 0.2 wt% Si. The RERTR-6 experiment tested fuel plates to moderate burnup, flux, and temperatures. The RERTR-7 experiment was a more aggressive experiment. During post-irradiation examination (PIE) of the fuel plates, destructive examinations were performed using optical metallography and, in some cases, scanning electron microscopy (SEM). For the SEM analysis, a scanning electron microscope was used to capture backscattered and secondary electron images of the microstructures of two samples taken from an irradiated fuel plate with 4043 Al alloy matrix and one sample taken from a plate with Al-0.2 wt% Si matrix. Attached wavelength-dispersive and energy-dispersive spectrometers (WDS/EDS) were employed to determine the amounts of various elements in the fuel, interaction zone, and matrix using x-ray mapping, linescans, and point-to-point analysis. This paper describes the results of the destructive examinations that were performed on the U-7Mo fuel with the highest Si (4043 Al) and lowest Si (0.2 wt%) matrices before and after irradiation, particularly focusing on the partitioning behavior of U, Mo, Al, and Si. Comparisons are made to some irradiation experiment results that have been reported for U-Mo dispersion fuels with only Al as the matrix.

2. FUEL PLATE FABRICATION AND CHARACTERIZATION

2.1 Fuel Plate Fabrication

The dispersion fuel for the RERTR-6 irradiation experiment was fabricated from powder produced by the Korean Atomic Energy Research Institute (KAERI) using a rotating-disk centrifugal atomization process.[9] The size distribution for the powder is enumerated in Table 1. For RERTR-7, the U-Mo powder produced at INL also uses the centrifugal atomization process.[10] The size distribution for this powder is presented in Table 2. A comparison of Tables 1 and 2 shows that the size distribution for the powder employed to fabricate RERTR-6 fuel plates differed greatly from what was used to fabricate RERTR-7 plates. The RERTR-6 powder had many fines, while the RERTR-7 powder had few fines and a much larger percentage of the powders in the 75-150 micron size range.

Table 1. The size ranges of the U-7Mo powders used to fabricate the dispersion fuel plates for the RERTR-6 experiment. The results are normalized by percentage.

Size Range (μm)	Percentage of powders in each size range for RERTR-6 plates
>150	0.01%
106–150	3.40%
75–106	22.34%
63–75	20.41%
45–63	24.91%
38–45	9.21%
<38	19.71%
Total Fines (<45μm)	28.93%

Table 2. The size ranges of the U-7Mo powders used to fabricate the dispersion fuel plates for the RERTR-7 experiment. The results are normalized by percentage.

Size Range (μm)	Percentage of powders in each size range for RERTR-7 plates
>150	0.0%
75–150	81.68%
63–75	8.22%
45–63	7.21%
<45	2.89

The dispersion fuel plates for the RERTR-6 irradiation experiment were fabricated at Argonne National Laboratory (ANL) in Illinois using a roll bonding process that had been used to fabricate earlier RERTR experimental fuels.[11] To make dispersion fuel meat, the U-7Mo powder was blended with 4043 Al alloy powder to have a target fuel loading of 6 g U/cm^3. The 4043 Al alloy powder had a composition, measured by chemical analysis, of 4.81Si-0.20Fe-0.14Ti-0.16Cu-0.01Cr-0.01Mn-bal Al. There was no Zn or Mg measured (<0,01 wt%). The blended powder was then formed under pressure into a compact. The compacts were placed in the cavity of a 6061 Al alloy "picture frame" and then cover plates were added to form the top and bottom cladding. This assembly was welded together and then rolled to form a plate of proper thickness. Specifically, the plates were hot rolled five passes at 500ºC for a reduction of approximately 85%. The plates were then cold rolled a further 10–15% (in two or three passes) to achieve

the final thickness, rough sheared, and shipped to INL for final processing. For the RERTR-7 fuel plates, all of these fuel plate fabrication steps were performed at INL.

The nominal fuel zone was rectangular, having a length of 8.1 cm, a width of 1.9 cm, and a uniform thickness of 0.06 cm. The 6061 Al cladding thickness for dispersion fuels is nominally 0.04 cm. The nominal fuel zone volume was therefore 0.957 cm^3. Uranium enrichment was specified to be 19.9% in the RERTR-6 fuel plates. To achieve the necessary surface heat fluxes that were being targeted as a part of the RERTR-7 experiment, which are characteristic of high-performance research reactors, the enrichment was increased to 58% ^{235}U for the U-7Mo powder.

2.2 Pre-Irradiation Characterization

During the fabrication campaign of the RERTR-6 irradiation experiment, some fuel plates were fabricated that were never placed in the reactor. These plates were used for characterization using SEM with EDS and WDS in order to identify the microstructure of fuel plates before irradiation. Fuel plate R3R020 was available for characterization to show the pre-irradiation microstructure of a U-7Mo/4043 Al alloy matrix dispersion fuel.

For the R3R020 sample, two different longitudinal cross sections were characterized. The representative microstructure of the first longitudinal cross section is presented in Figure 1, which clearly shows a wide range in the sizes of the atomized powders. This is in good agreement with the sieve analysis results reported in Table 1.

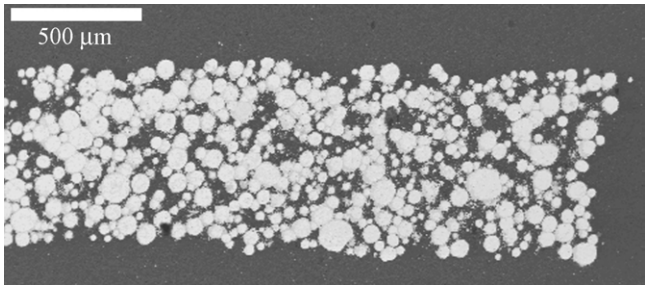

(a)

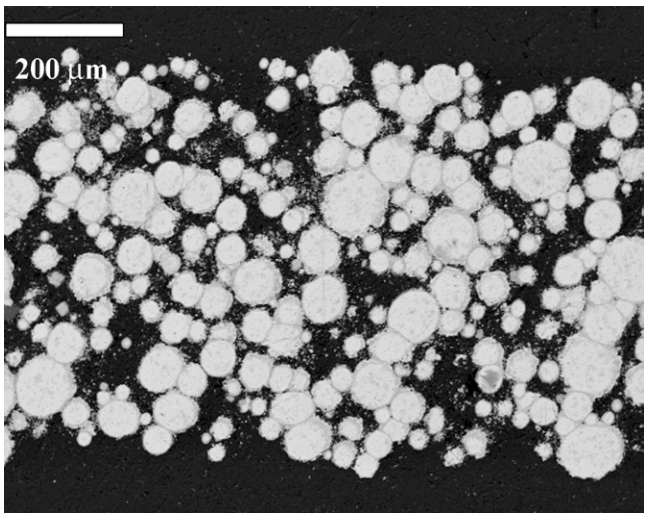

(b)

Figure 1. Backscattered electron images of one-half of a transverse cross-section taken from fuel plate R3R020, which had U-7Mo fuel particles dispersed in 4043 Al alloy matrix. The center of the fuel plate is to the left in (a).

A more detailed characterization of the U-7Mo powders (see Figure 2) showed that after the five rolling passes at 500°C which the plates were subjected to during fabrication, and after the blister anneal testing that occurred after hot rolling (485°C for ~60 minutes), noticeable fuel/matrix interaction had occurred. The blister anneal is run to demonstrate that blisters do not form on the surface of a fuel plate because of inadequate bonding between the fuel meat and the 6061 Al alloy cladding. The same fuel/matrix interaction was observed in the other longitudinal cross section.

The result of the fuel/matrix interaction was the formation of a fairly uniform layer around each particle, along with localized areas where the rate of interaction was greatly enhanced. There appeared to be interaction product that formed along grain or phase boundaries into the fuel particles. At a temperature near 500°C, it has been demonstrated that γ-phase U-7Mo alloy will decompose to α-U and γ' (U_2Mo) in less than an hour.[12] Such decomposition results in high diffusion rates at the grain boundaries where the α-U develops, since α-U interdiffuses with Al at a relatively high rate.[13] This explains why Al penetrates furthest along the grain boundaries (see Figure 2b). Figure 2c shows that Si particles were present in the as-fabricated fuel. Si can show up in the fuel particles as an impurity.

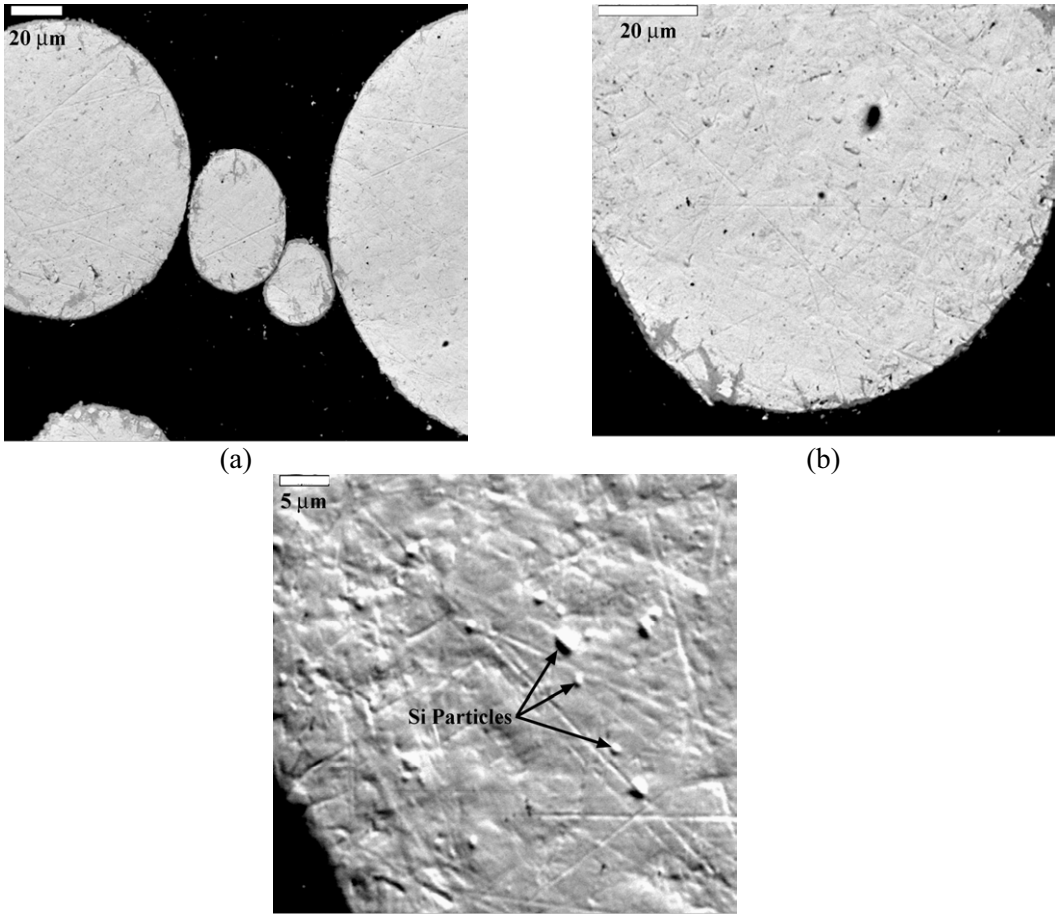

Figure 2. Backscattered electron images (a,b) showing the interaction phases (medium contrast) that formed in R3R020 during fabrication. The areas bright in contrast are the U-7Mo fuel. The medium contrast regions are interaction product. The black areas are the 4043 Al alloy matrix. Si particles that were present in the U-7Mo powder as an impurity are identified in (c).

X-ray maps were generated for R3R020 to determine how the various fuel and matrix constituents partitioned between the fuel, interaction layer, and matrix (see Figure 3) during fuel plate fabrication. Based on these x-ray maps, it can be seen that the interaction layer was enriched in Si. U, Mo, and Al were also present in the layer. Oxygen was not enriched in the interaction layer.

Point-to-point SEM/EDS analysis was performed on the interaction layer that surrounded the fuel particle shown in Figure 3a. The results of this analysis indicated that the interaction layer had a Si content of up to 45 at%, the maximum (Al + Si) concentration was 69 at%, and the (Al+Si)/(U+Mo) ratio varied between 1.7 and 2.2.

Two as-fabricated fuel plates with 4043 Al matrices were characterized as part of the RERTR-7 experiment fuel fabrication campaign. One had U-7Mo-1Ti fuel particles and the other had U-7Mo-2Zr. However, titanium (Ti) and zirconium (Zr) are being looked at as an addition to the U-Mo fuel alloy that may reduce fuel/matrix interactions during irradiation.[4] As was expected based on a sieve analysis, a higher fraction of the U-7Mo particles was observed to be of a large size overall in these plates in comparison to the R3R020 plate (see Figure 4), and Si-rich interaction layers were observed to have formed around the fuel particles during fabrication (see Figure 5).

No fuel plates with an Al-0.2 wt% Si matrix were available for characterization after fabrication due to the aggressive schedule that had to be met to get fuel plates into the reactor for testing. However, diffusion studies have been performed at 500°C using alloys with low amounts of Si,[5] and it has been demonstrated that Si-rich layers will form during short-term anneals between U-7Mo and low-Si alloys.

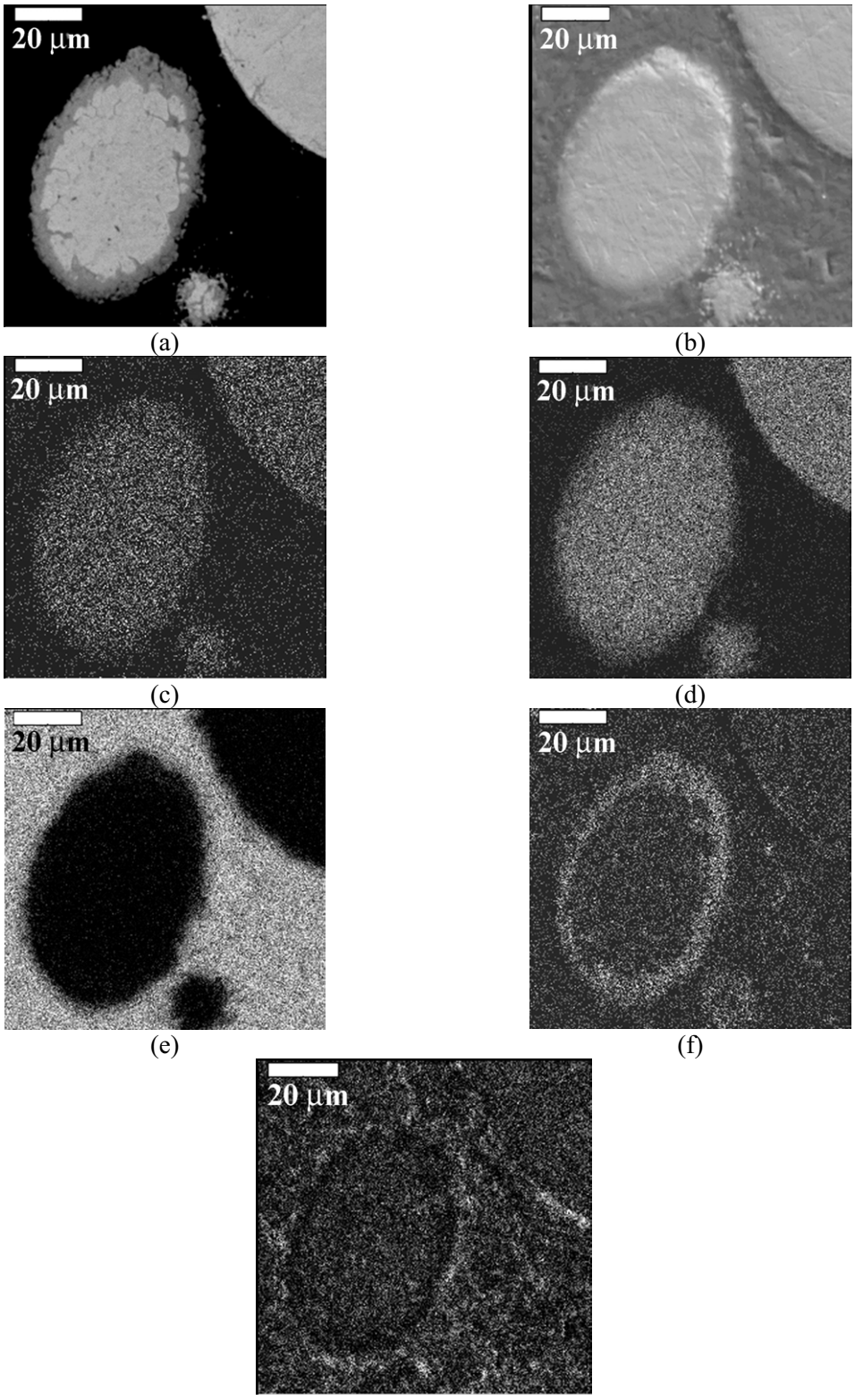

Figure 3. Backscattered and secondary electron images (a,b) and x-ray maps for (c) Mo, (d) U, (e) Al, (f) Si, and (g) oxygen taken for sample R3R020.

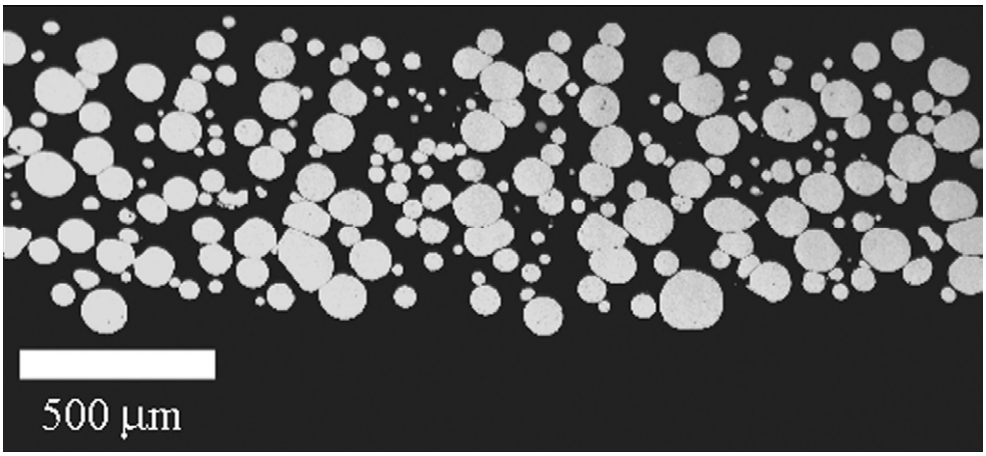

(a)

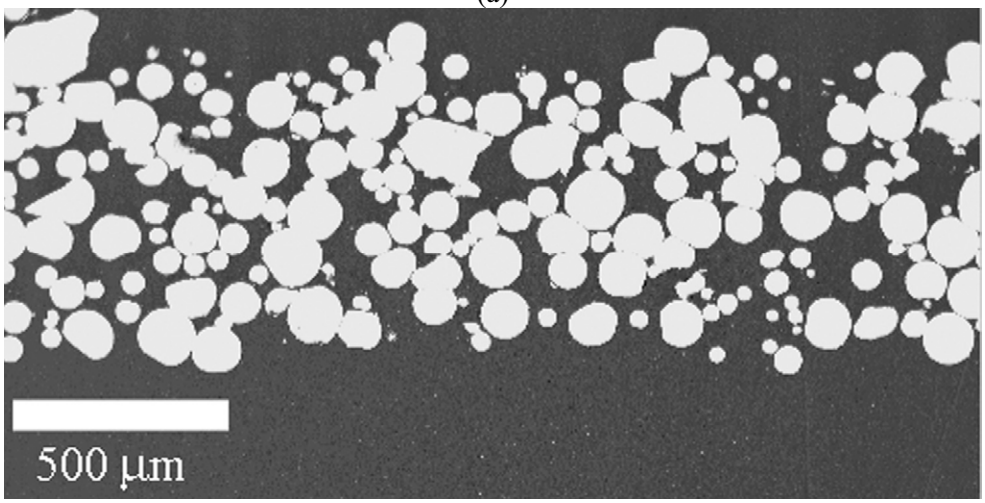

(b)

Figure 4. SEM micrographs of as-fabricated RERTR-7 fuel plate microstructures with (a) U-7Mo-2Zr and (b) U-7Mo-1Ti particles.

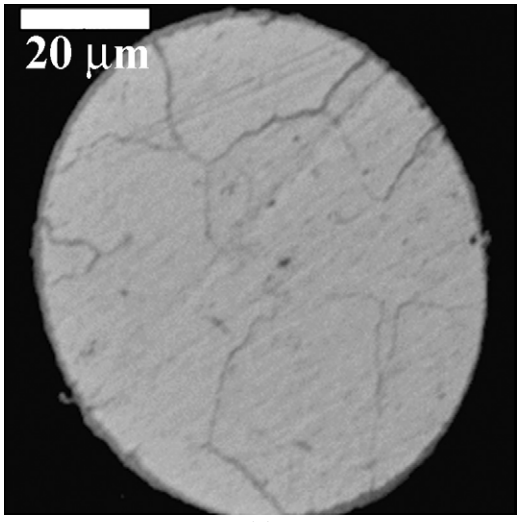

(a)

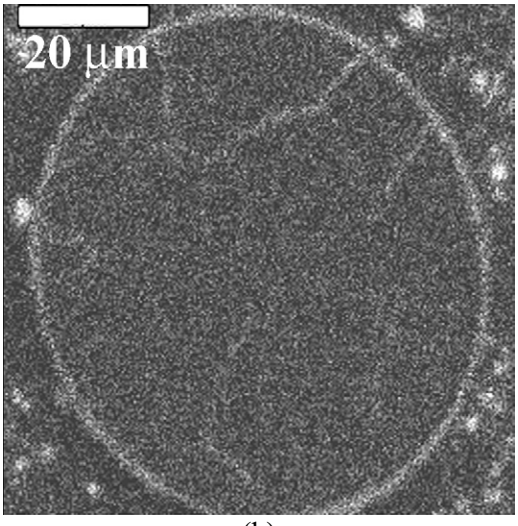

(b)

Figure 5. Backscattered electron image (a) and Si x-ray map for the (b) RERTR-7 U-7Mo-2Zr sample with 4043 Al alloy matrix.

3. IRRADIATION TESTING

The RERTR-6 experiment tested fuel materials to high burnup under moderate flux and moderate temperature conditions. The experiment was irradiated in the ATR West B-12 irradiation test position during cycles 134B, 135B, and 135C, and it remained in the reactor for 135.1 effective full-power days (EFPD). The RERTR-6 irradiation test assembly held four capsules, axially designated as A through D, from the top of the test assembly to the bottom. Each capsule had two levels, with four mini-plate positions per level, giving eight mini-plate positions per capsule. There were 32 mini-plate positions per test assembly (four capsules with eight mini-plate positions per capsule). Table 3 lists peak temperature, average burnup, average fission density, average fission rate, and peak heat flux for the RERTR-6 fuel plates R30R030, which was comprised of U-7Mo particles in 4043 Al alloy matrix, and R5R020, which employed an Al-0.2 wt% Si matrix. Due to the orientation of the fuel plates, where one edge of each fuel plate faced the core, there was a large neutron flux gradient across the width of the plate. Figure 6 shows an example of the neutron flux gradient across the width of RERTR-6 fuel plate R3R030.

The RERTR-7 experiment was a more aggressive test. To achieve the necessary surface heat fluxes (which correlate with fission rate density) characteristic of what are considered the high-performance research reactors (e.g., ATR), the enrichment for the RERTR-7 experiment was increased to 58% ^{235}U. The experiment was divided into two parts: RERTR-7A and RERTR-7B. The 7A experiment was loaded into the ATR in November 2005 in experimental position B-11 for cycles 136A and 136B. It remained in the ATR for both cycles for 90 EFPD. Average burnup of the 58%-enriched fuel was 21 to 30% ^{235}U, depending on the location in the experiment. When converted to an LEU equivalent to facilitate comparison with RERTR-6 data and other LEU experiments, average burnup was 62 to 89% LEU equivalent. Beginning-of-Life (BOL) fuel temperatures were <225°C, and the peak heat flux was 325W/cm^2. The R3R040 and R3R050 samples described in this paper (see Table 3) were included in RERTR-7A. Like the RERTR-6 experiment, the RERTR-7A experiment basket was positioned so that one edge of the miniplates faced the core. As a result, a strong neutron flux gradient existed across the width of the fuel plates. The higher enrichment in RERTR-7 increased the contribution of self-shielding, and, consequently, the high-flux edge ran approximately two times the power of the low-flux edge. Figure 6 shows the fission density and fission-rate gradients across the width of the RERTR-7 fuel plate R3R040.

Table 3. Calculated values for peak temperature, average fission (f) density, average fission rate, and peak heat flux for the overall fuel plates R3R030, R5R020, R3R040, and R3R050.

Sample	Matrix	Peak Plate Temperature (˚C)	Ave. Fission Density (10^{21} fcm^{-3})	Ave. Fission Rate (10^{14} fcm^{-3}s^{-1})	Peak Heat Flux for entire plate (W/cm^2)
R3R030	4043 Al[a]	97.5	3.26	2.80	101.5
R5R020	Al-0.2Si	117.1	3.30	2.83	130.5
R3R040	4043 Al	ND[b]	5.03	6.46	ND
R3R050	4043 Al	139.9	4.90	6.30	299.3

a. The 4043 Al alloy was measured by chemical analysis to have a composition, in wt%, of 4.81Si-0.20Fe-0.14Ti-0.16Cu-0.01Cr-0.01Mn. Less than 0.01 wt% of Zn and Mg was measured.

b. Not Determined.

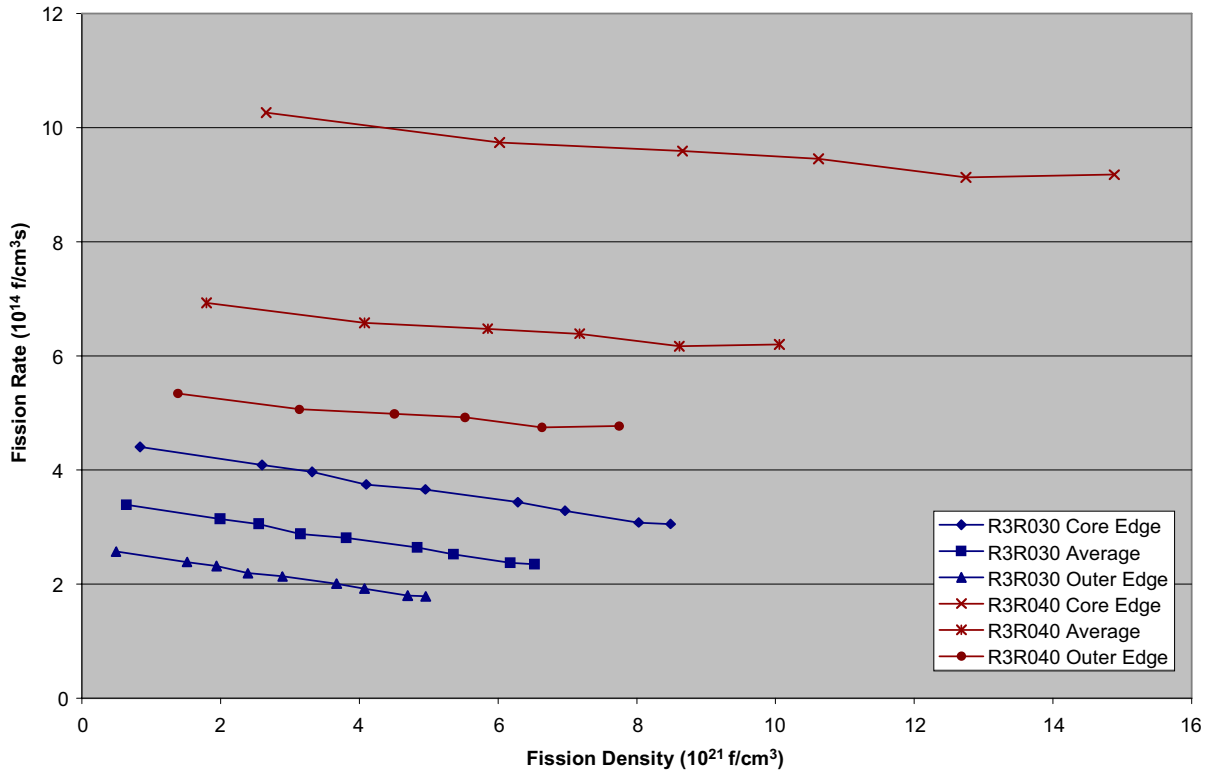

Figure 6. Fission (f) rate history for plates R3R030 (RERTR-6) and R3R040 (RERTR-7A) at the core edge and outer edge. A large neutron flux gradient was observed across the width of the plates, especially for the plate irradiated as part of the RERTR-7 experiment.

4. POST-IRRADIATION EXAMINATION

4.1 Optical Metallography

4.1.1 R3R030

After irradiation of the various fuel plates, microstructural analysis was performed using an optical metallograph. Plates were mounted in epoxy, polished through 1200-grit, and examined in the etched and unetched condition. Complete transverse cross sections of the plates were characterized. Figure 7a shows the microstructure of a complete cross section of RERTR-6 fuel plate R3R030 and some images at higher magnification. The side of the plate exposed to the highest neutron flux is labeled "hot," and the edge exposed to the lowest flux is labeled "cold." A comparison of Figures 7b and 7c with Figure 1b shows that the interaction layers present in this fuel plate, irradiated under the conditions of the RERTR-6 experiment, are very similar to those observed in a fuel plate after fabrication. This applied to both the hot and cold edges of the fuel plate.

4.1.2 R3R040

Fuel plate R3R040 was the first of two RERTR-7 fuel plates with 4043 Al alloy matrix that were characterized using optical metallography. Low- and high-magnification images of the fuel plate microstructure are presented in Figure 8. Interaction layers were observed around the U-7Mo particles, with a maximum observed thickness of around 10 μm. Overall, the layers were thicker than those observed for R3R030. In the area of the transverse cross section that was exposed to the highest burnup, porous regions could be identified. Recall that Table 3 showed this plate was irradiated at a much higher fission rate and to a higher fission density than R3R030.

4.1.3 R3R050

Plate R3R050 was the final RERTR-7 dispersion fuel plate with 4043 Al alloy matrix that was characterized using optical metallography. Figure 9 shows the microstructure that was observed for this fuel plate. Like R3R040, this fuel plate displayed interaction layers that were thicker than those observed for R3R030. The maximum interaction layer thickness was around 10 μm.

4.1.4 R5R020

The only characterized fuel plate that had an Al-0.2 wt% Si matrix was R5R020, which was irradiated in the RERTR-6 experiment. The optical micrographs that were taken of sample R5R020 (see Figure 10) show that appreciable fuel/matrix interaction had occurred in this fuel plate. These interaction layers are more significant than those that developed in the irradiated fuel plates with 4043 Al alloy matrix. Pores developed in the high-burnup region of the plate and appeared to be linking up, as shown to the right of Figures 10a and 10d. Figure 10e shows a higher magnification image of the porous microstructure.

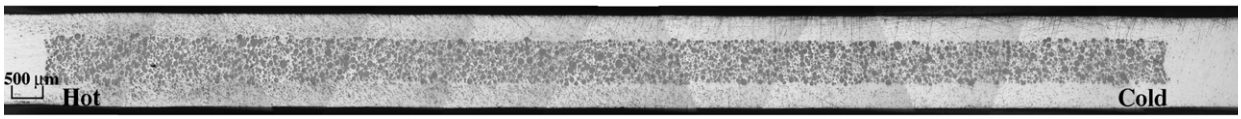

(a)

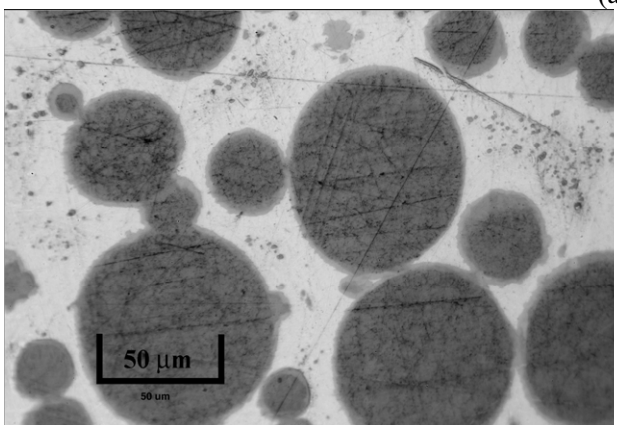

(b)

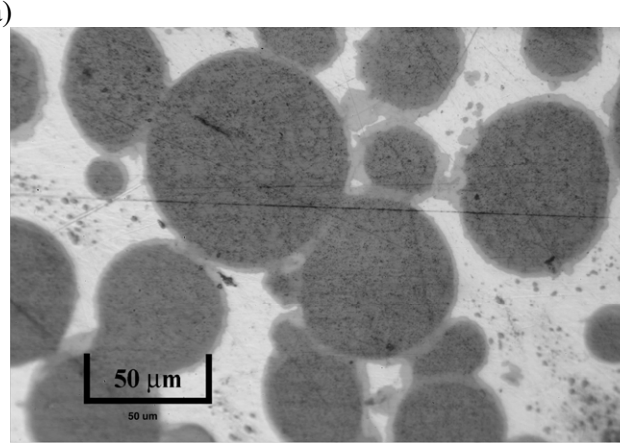

(c)

Figure 7. Optical micrographs of (a) the microstructure of a transverse cross section taken at the midplane of fuel plate R3R030, (b) the microstructure in an area near the "hot" edge of the plate, and (c) the microstructure near the "cold" edge of the plate.

Cold 500 µm Hot

(a)

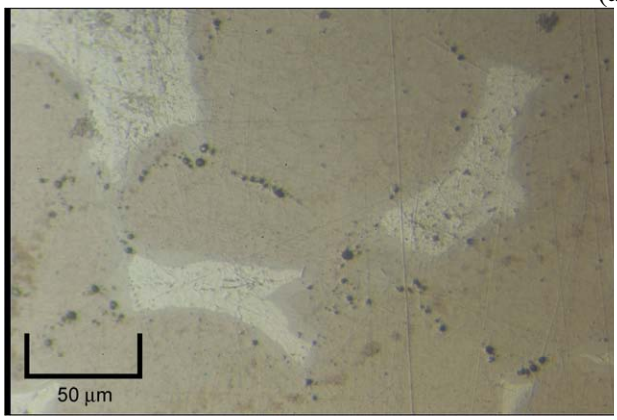

(b)

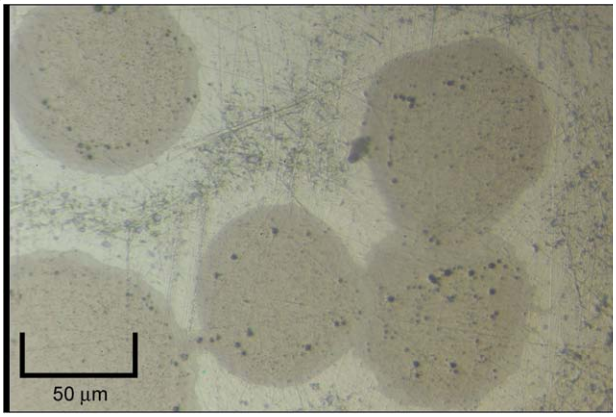

(c)

Figure 8. Optical micrographs of (a) the microstructure of a transverse cross-section taken at the midplane of fuel plate R3R040, (b) the microstructure in an area near the "cold" edge of the plate, and (c) an area near the "hot" edge of the plate.

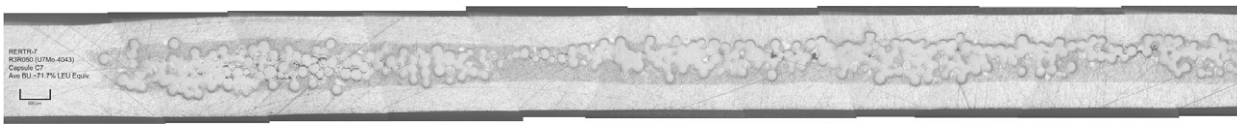

(a)

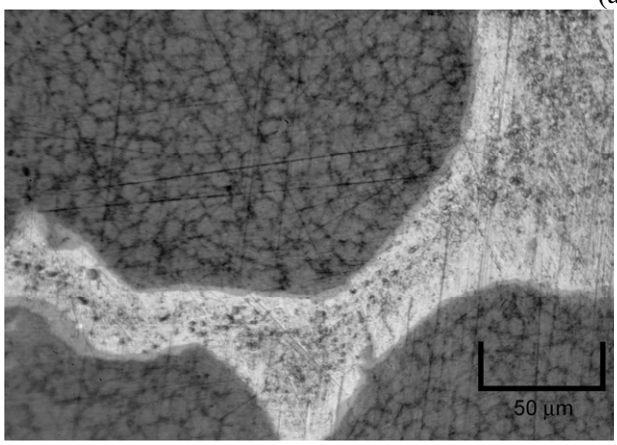

(b)

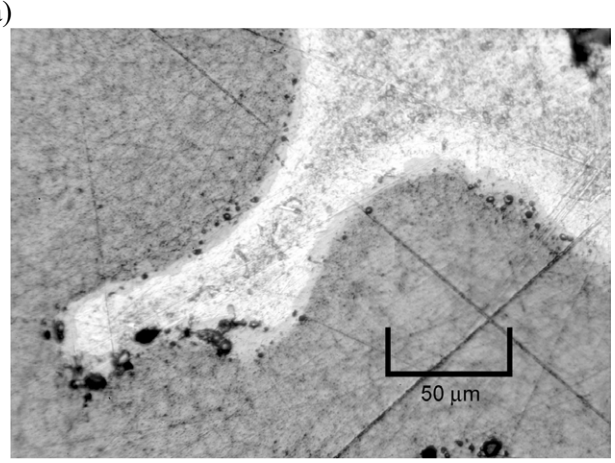

(c)

Figure 9. Optical micrographs of (a) the microstructure of a transverse cross-section taken at the midplane of fuel plate R3R050, (b) the microstructure in an area near the "cold" edge of the plate, and (c) an area near the "hot" edge of the plate.

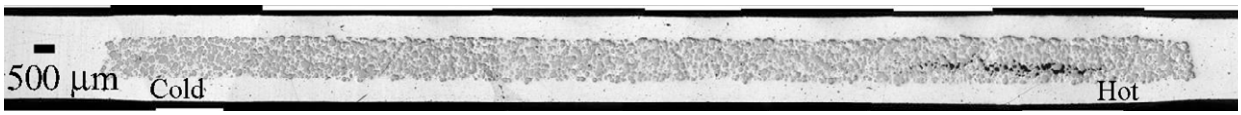

(a)

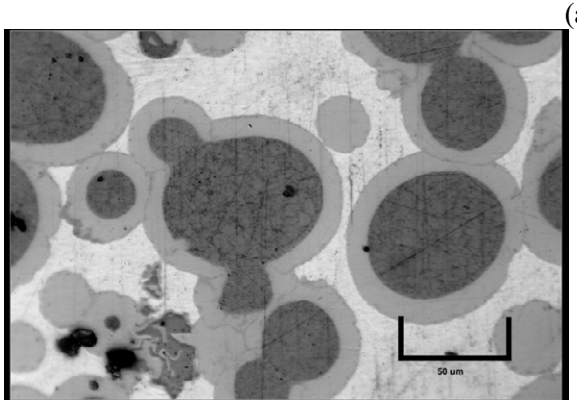

(b)

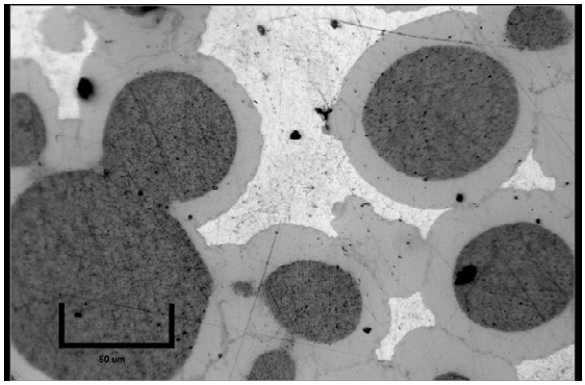

(c)

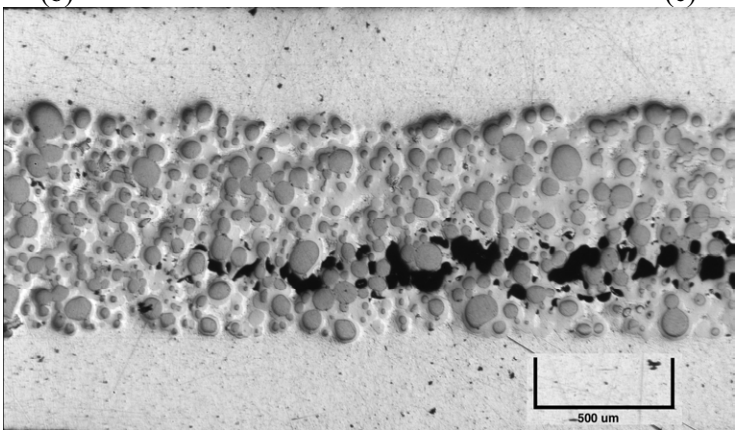

(d)

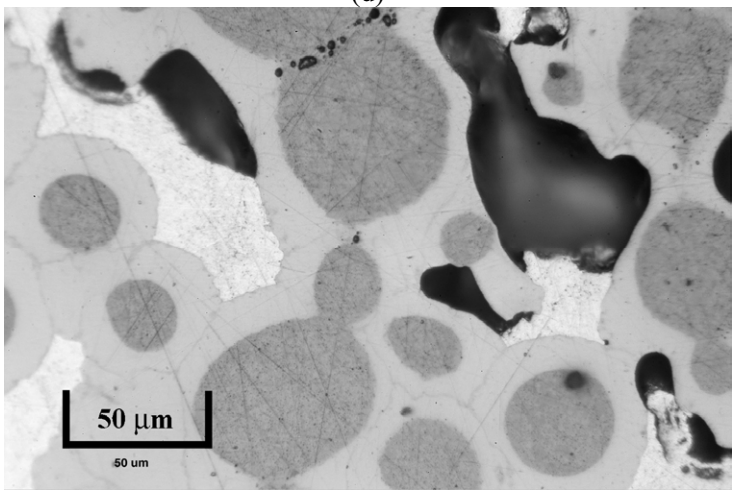

(e)

Figure 10. Optical images of R5R020, where (a) is a complete transverse cross-section at the midplane, and (b) and (c) were taken at relatively low and high flux regions of the plate, respectively. (d) is a blown-up area of the porous region shown in (a). (e) is a high magnification image of the fuel microstructure around some of the large pores.

4.2 Scanning Electron Microscopy

4.2.1 R3R030A

Two punchings (labeled R3R030A and R3R030B) were generated from the R3R030 fuel plate for SEM analysis. In the Hot Fuel Examination Facility (HFEF), a commercially available press that had been modified for easier operation in a hot cell environment was used to produce 1-mm-diameter cylindrical punchings taken through the nominally 1.9-cm-wide fuel meat.[14] The samples were transferred to the Electron Microscopy Laboratory for sample preparation and analysis. Since this analysis took place approximately 1.5 years after the fuel plates had been discharged from ATR, handling of these relatively small samples was manageable in this facility. In an air glovebox, the punchings were mounted longitudinally in a phenolic ring using an epoxy mixed with 325-mesh tungsten powder to provide shielding. The samples were then polished through 1200-grit sandpaper. The mounted samples were coated with palladium (Pd) and then inserted into a ZEISS Model 960A SEM that was equipped with an Oxford WDS and EDS that employed ISIS LINK software. Backscattered electron and secondary electron images were generated to examine the fuel microstructural features, and the WDS and EDS spectrometers were employed to generate x-ray maps, linescans, and to perform point-to-point compositional analysis to determine the presence of various elements in the fuel, interaction zone, and matrix.

Based on the optical micrographs taken of fuel plate R3R030, the microstructure for the punchings should be comprised of U-7Mo particles with approximately 1- to 2-μm-thick interaction layers around the fuel particles. Figure 11 shows an SEM image of the microstructure that was observed for sample R3R030A. Higher magnification images (see Figure 12) show that narrow interaction layers are present around the fuel particles. X-ray mapping was employed using WDS to identify the partitioning behavior of the U, Mo, Al, and Si (see Figure 13). U, Mo, Al, and Si are observed in the interaction layers. Si is also found in precipitates in the 4043 Al alloy matrix. Around the fuel particles, there are regions that are devoid of Si precipitates. This is probably because recoil zones are present around the fuel particles during irradiation,[15] and these regions extend about 10 μm into Al. This causes the original Si-rich precipitates to dissolve, leaving behind precipitate-free-zones (PFZ). Since Si behavior is of particular interest in these fuels, higher magnification x-ray mapping was performed to specifically investigate Si partitioning behavior in the interaction layers. A high magnification Si x-ray map is presented in Figure 14, which shows that most areas of the interaction layers were enriched in Si; however, some areas appear to be more enriched than others, suggesting that the layers may consist of more than one phase or a phase with a large range in Si concentration. Typically, point-to-point composition analysis would be performed to determine the composition of the Si-rich interaction layer, but due to the narrow thickness of the layer, a reliable phase composition could not be determined.

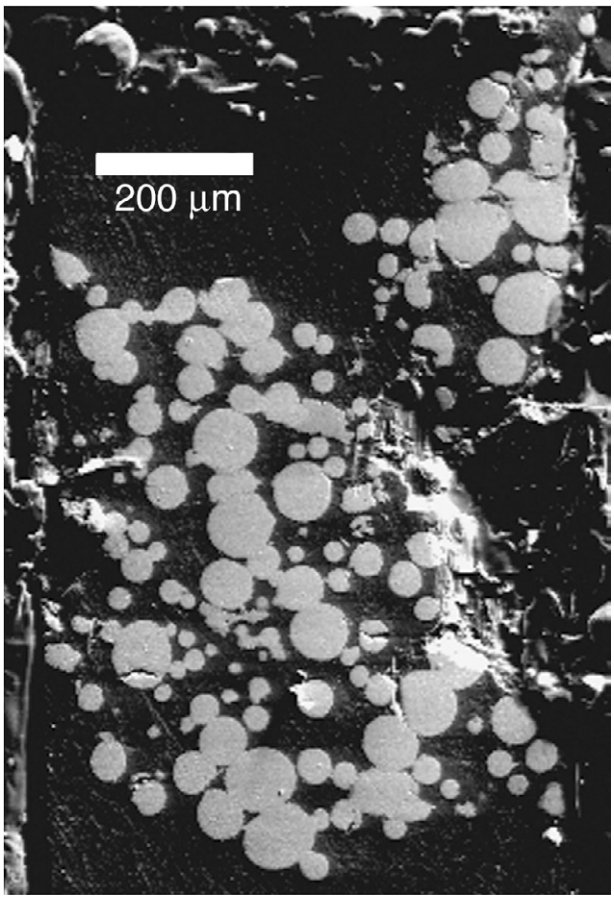

Figure 11. Secondary electron image of the microstructure for a longitudinal cross section taken through sample R3R030A. The bright contrast phases are U-7Mo particles contained in 4043 Al matrix.

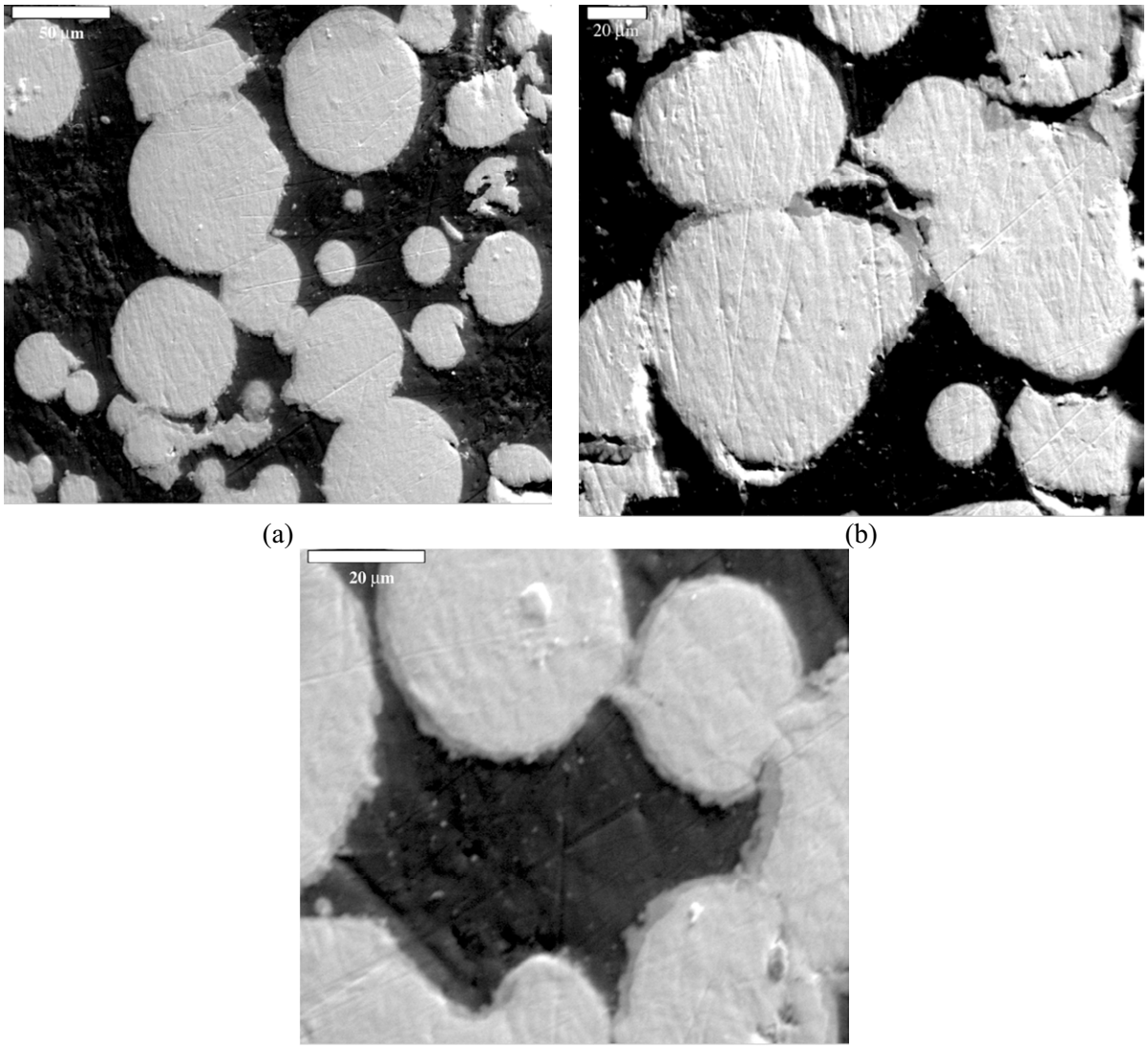

Figure 12. SEM images of the microstructure for sample R3R030A where relatively thin interaction layers (medium gray) were observed around the U-7Mo (bright contrast) particles.

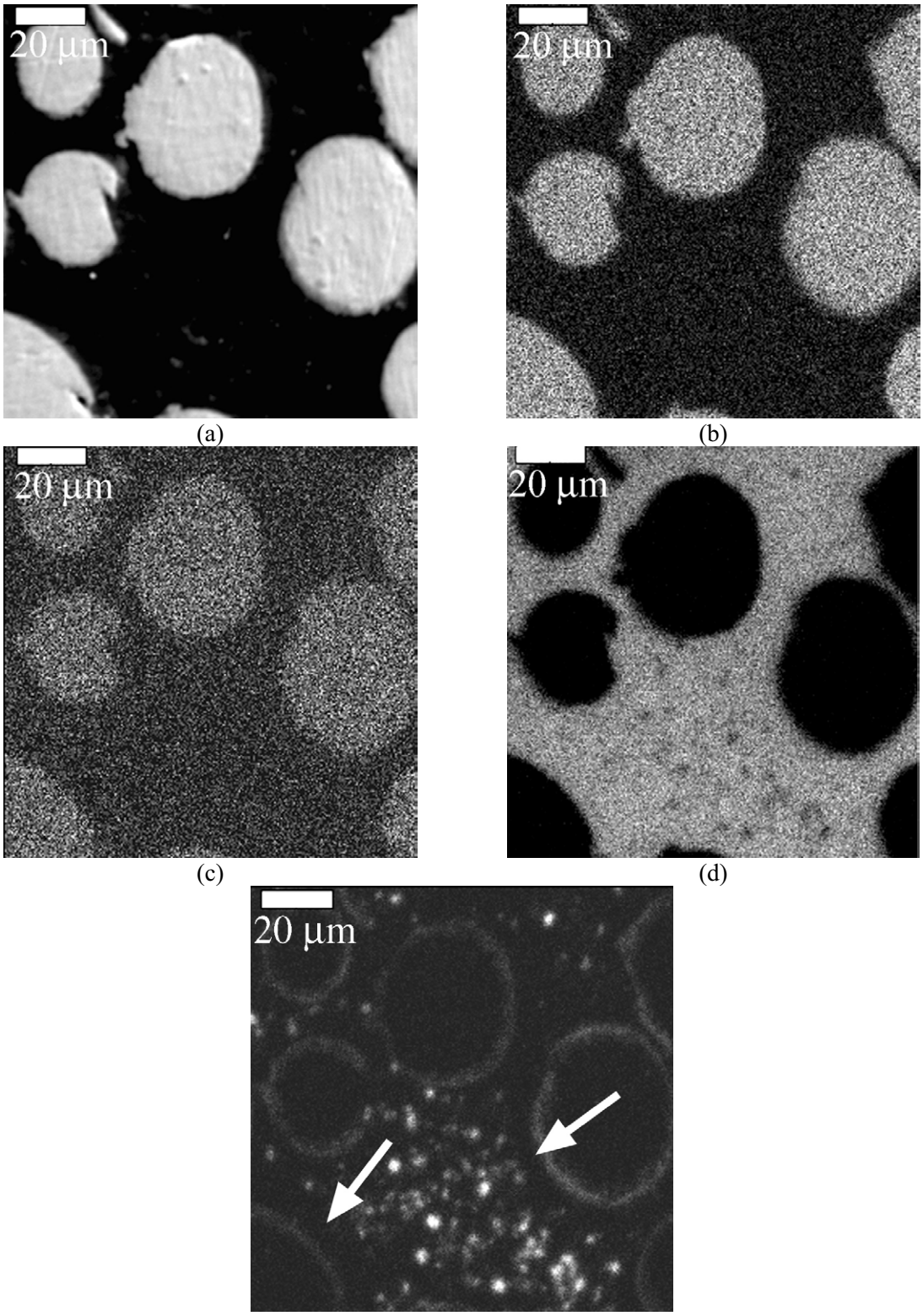

Figure 13. SEM image (a) and x-ray maps for (b) U, (c), Mo, (d) Al, and (e) Si for the R3R030A sample. The arrows in (e) indicate PFZ in the microstructure.

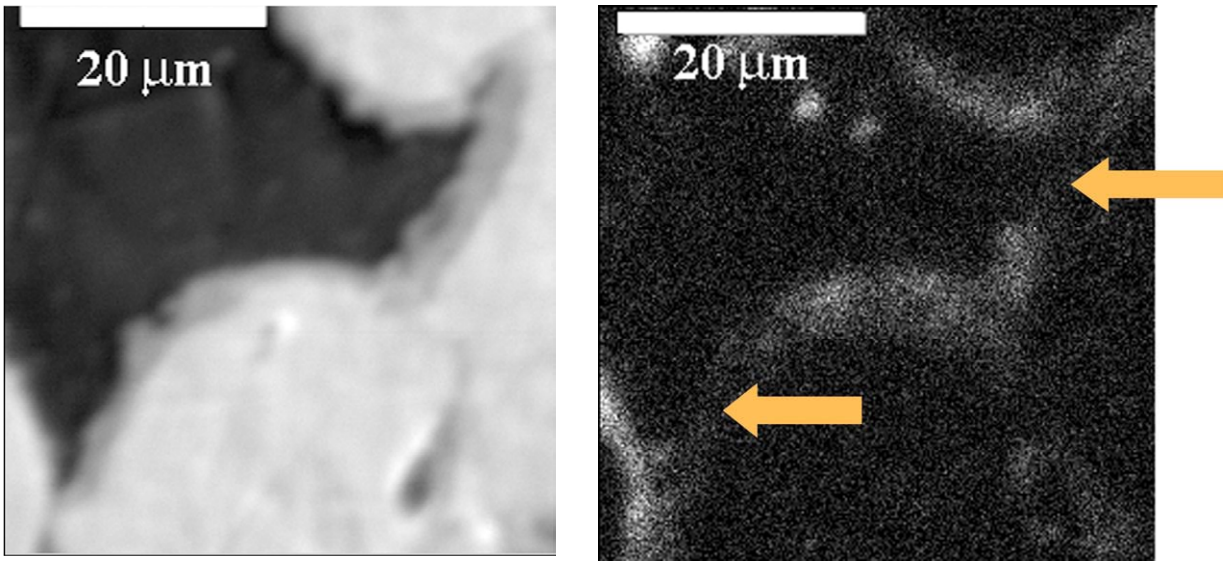

(a) (b)

Figure 14. SEM image (a) and Si x-ray map (b). The arrows in (b) identify the areas in the interaction zone where Si is depleted.

4.2.2 R3R030B

An SEM image of the microstructure observed for sample R3R030B is presented in Figure 15. The microstructure in this sample is different than the one for sample R3R030A. Based on the microstructure seen in optical micrographs (see Figure 7) and SEM micrographs for sample R3R030A, only U-7Mo particles with narrow interaction layers should be observed; however, this is not the case for sample R3R030B. Instead, the microstructure is comprised of U-7Mo particles with relatively wide interaction zones, and non-spherical "islands" are also present. These islands may be due to the punching process, which may have affected the microstructure of the fuel zone towards the edges of the sample by displacing some of the fuel particles and interaction zone. On the other hand, the non-spherical particles may have already been present in the starting powder given that a reasonably high fraction of "fines" (over 28%) was present amongst the original U-Mo powder.

Apparently, at the center of the punching, some fuel particles were only minimally affected. These particles had a morphology that was similar to the overall fuel plate microstructure and were selected as the best candidates for detailed characterization. Figure 16 shows a higher magnification image of the fuel particles that were present at the center of the punching. The largest particle available for analysis in this sample is on the order of 80 to 100 μm in diameter. Based on Table 3, only 3% of the U-7Mo powders used to fabricate this plate would have been larger than this particle. Therefore, this sample allowed for characterization of what would be considered large and small U-7Mo fuel particles. In addition, based on the large size of the particle shown in Figure 16, there is a reasonable chance that the surface being exposed for this particle is near its midplane. Based on contrast variation, which is a function of the atomic number of the material in an electron micrograph, there are two different composition regions associated with the fuel particles. In Figure 16a, one region is labeled "U-7Mo" and the other is labeled "Interaction Zone." Composition analysis data, which will be discussed later, confirms this.

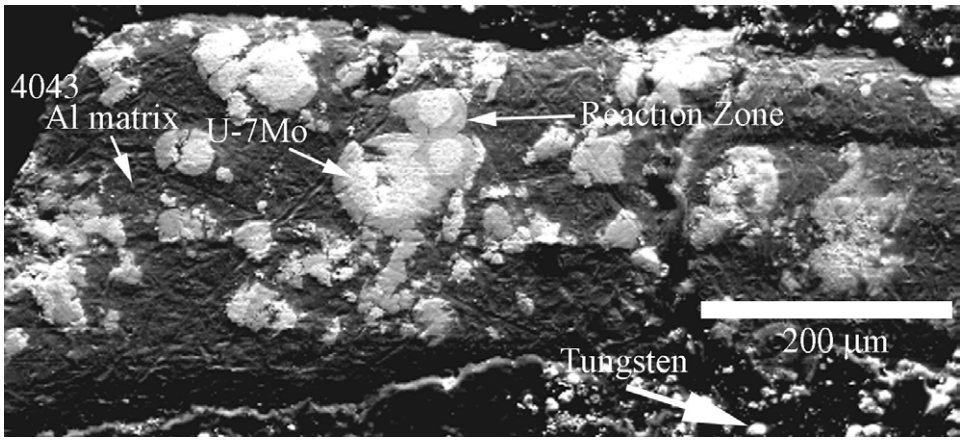

Figure 15. A low-magnification secondary electron image sample R3R030B. The tungsten that is observed is a part of the sample mount and was added to provide shielding.

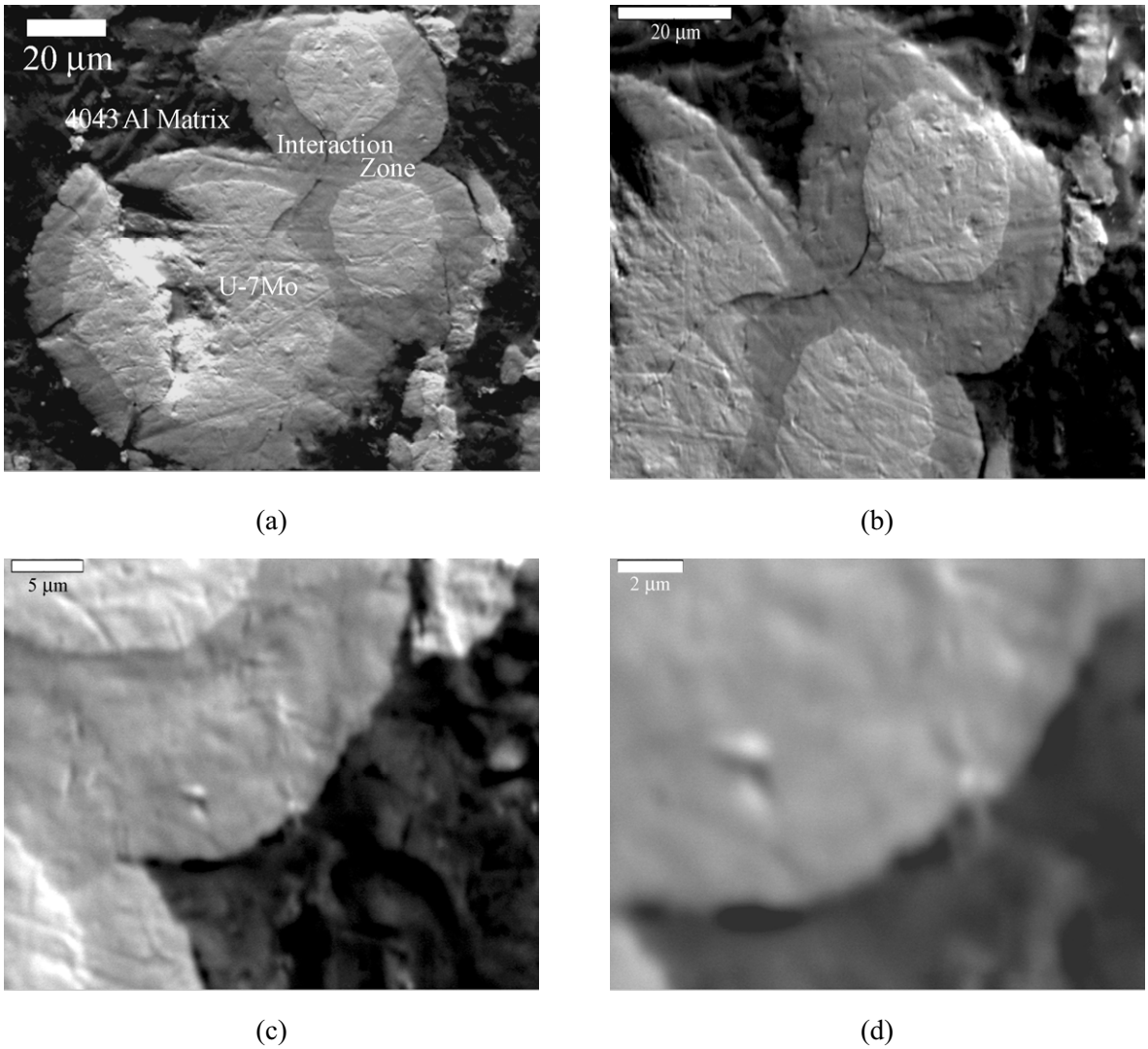

(a) (b)

(c) (d)

Figure 16. Secondary electron images of fuel particles and interaction zones observed toward the center of sample R3R030B.

The size of porosity that develops in irradiated fuel is of interest because it will contribute to the overall swelling behavior of the fuel plate, so high magnification images were generated for various particles in the R3R030 sample and are presented in Figures 16c and 16d. Careful analysis of the fuel particles and interaction zones did not reveal any significant signs of porosity in either phase. Because the SEM samples were polished through 1200-grit, smearing of the porosity was a possibility. To limit personnel exposure, the time spent polishing had to be limited, and it appears that better polishing will be required to expose fission gas porosity.

As was the case for the as-fabricated fuel (see Figure 2c), a dark-contrasted phase was observed in the irradiated U-7Mo particles, as shown in Figure 17. Composition analysis using WDS showed the phase to be enriched in Si, with negligible oxygen or carbon. This phase seems to be identical to the one observed in the original as-fabricated fuel. Si was a minor impurity present in the original powder, and the irradiation process has caused little change in composition or morphology of this phase.

X-ray maps were generated using WDS to identify the partitioning behavior of U, Mo, Al, and Si within sample R3R030B. Both low- and high-magnification x-ray maps were produced. Figure 18 shows some low-magnification x-ray maps that were generated in a region of the fuel where the largest U-7Mo particle was present in the sample. Figure 19 shows higher-magnification x-ray maps. U, Mo, and Al are observed to be present in the interaction layer that forms in this sample. U and Mo are observed in the fuel; Al and Si are not. In the interaction layer, uniform concentrations of U, Mo, and Al are present. Figure 19 indicates that there are no concentration gradients for any of the constituents. Negligible Si is observed in the interaction layer. Instead, Si was mainly observed in the Si-rich precipitates that are associated with the 4043 Al alloy cladding. Some Si was found in the particles mentioned earlier that appeared to be a contaminant in the fuel. Since iron (Fe) is another constituent present in the 4043 Al alloy matrix, the partitioning behavior of this constituent was also determined using x-ray mapping (see Figure 20).

The thickness of the interaction layers in sample R3R030B was adequate for point-to-point EDS analysis to be performed. Figure 21 shows the exact locations within the layer where the data was taken. The results of this analysis are presented in Table 4. The minimum atomic percent values for Al, Mo, and U were 80.6, 1.6, and 14.2, respectively. The maximum atomic percent values for Al, Mo, and U were 83.6, 3.7, and 16.3, respectively. The mean atomic percent values for Al, Mo, and U were 82.4, 2.5, and 15.1, respectively. The standard deviations were 1.0, 0.6, and 0.6 for the Al, Mo, and U atomic percent values, respectively. Overall, the data points within the interaction layer showed good agreement. Based on the data in Table 4, the interaction layers that formed during irradiation, in the local area of fuel plate R3R030 where R3R030B was taken, had a composition near that of the $(U,Mo)_{0.9}Al_{4.4}$-type phase depicted in the U-Al phase diagram.[16]

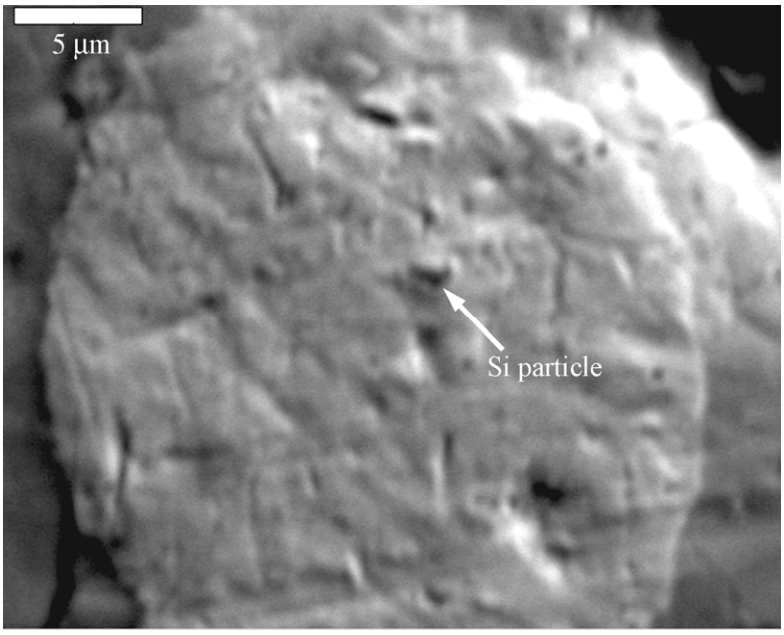

Figure 17. Secondary electron images of U-7Mo fuel surrounded by an interaction layer. Si particles were observed in some areas of the U-7Mo particles.

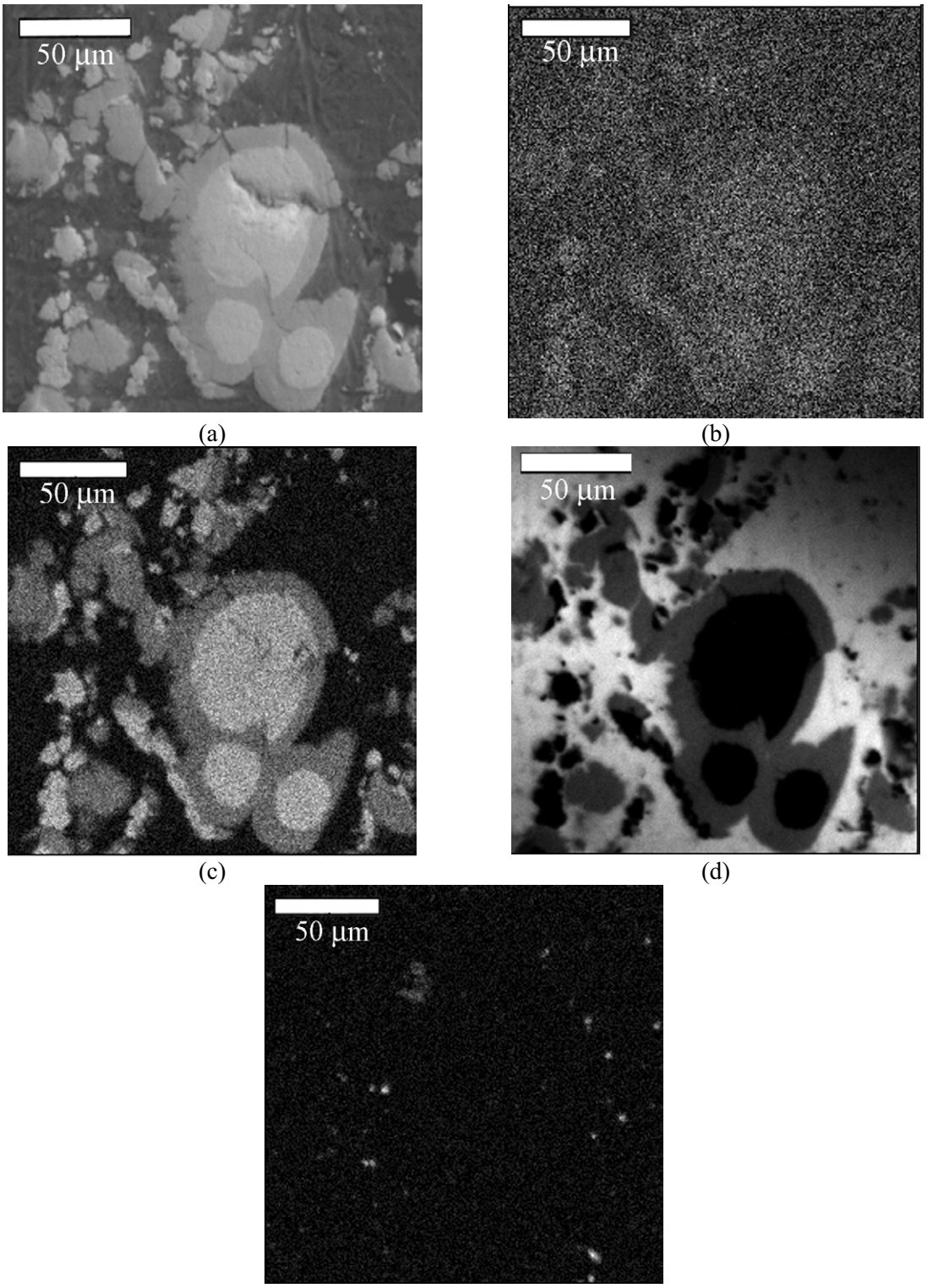

Figure 18. Secondary electron image (a) and x-ray maps for (b) Mo, (c) U, (d) Al, and (e) Si taken for sample R3R030B.

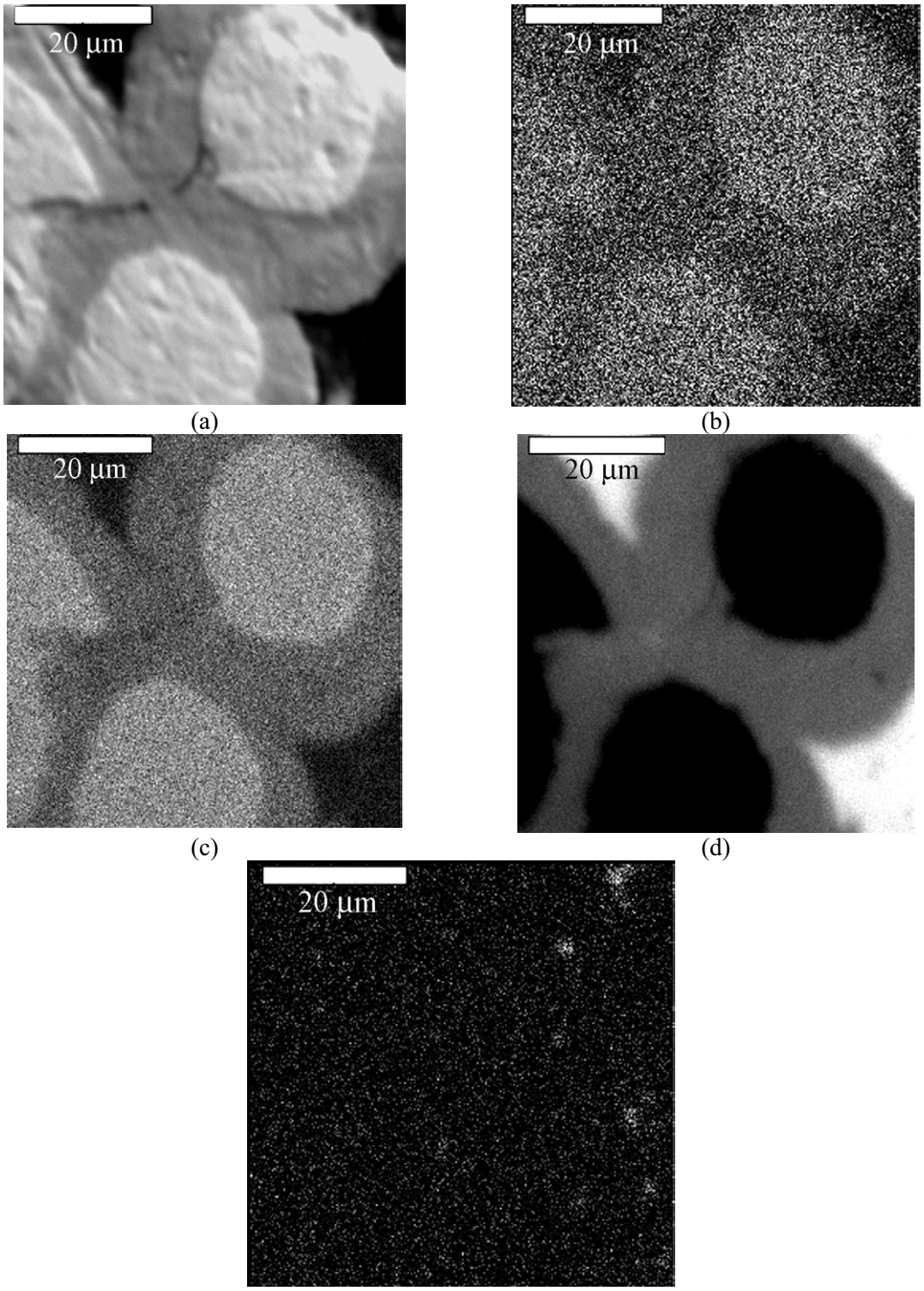

Figure 19. Secondary electron image (a) and x-ray maps for (b) Mo, (c) U, (d) Al, and (e) Si taken for sample R3R030.

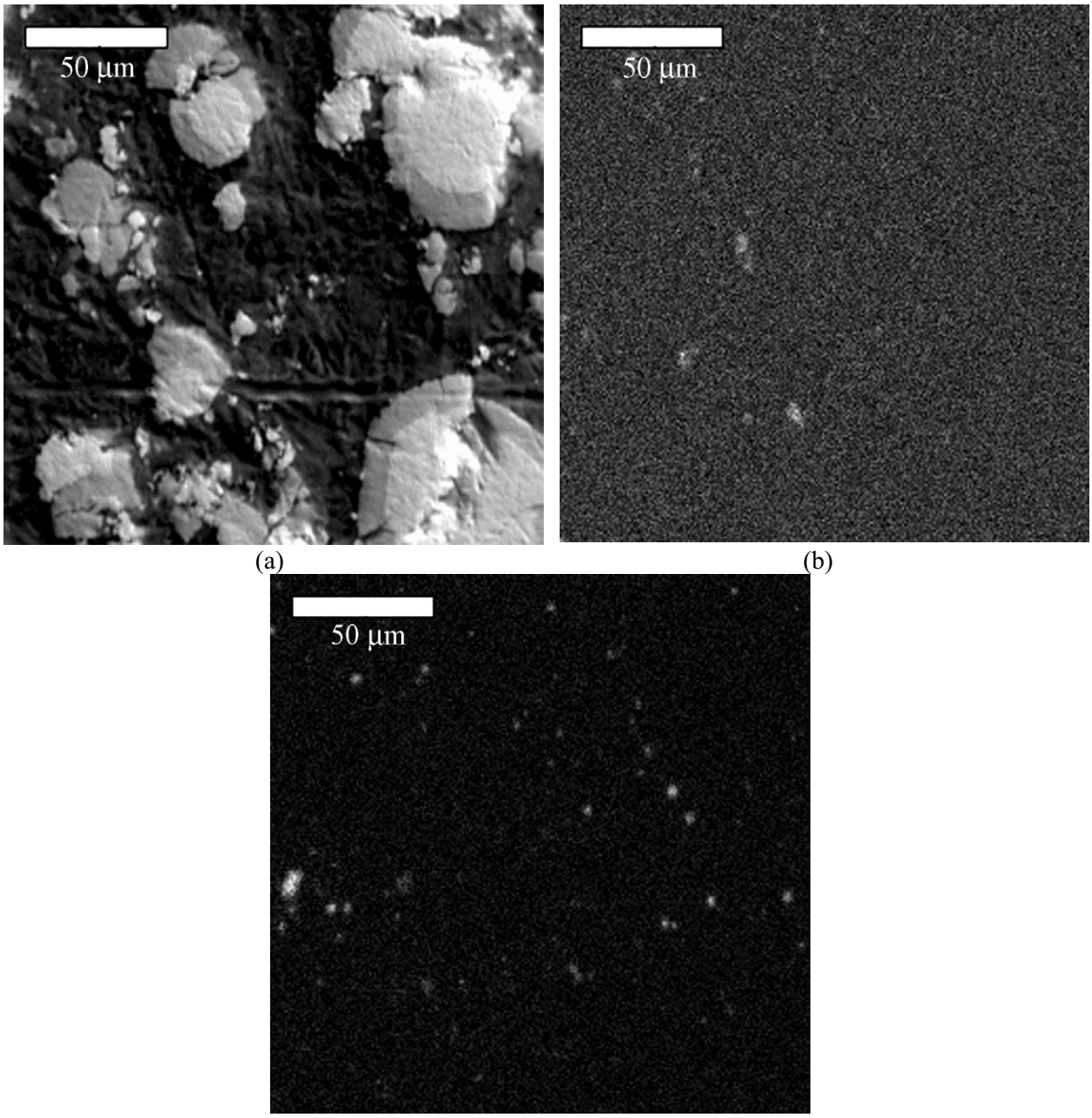

(a) (b)

(c)

Figure 20. Secondary electron image (a) and x-ray maps for (b) Fe, and (c) Si.

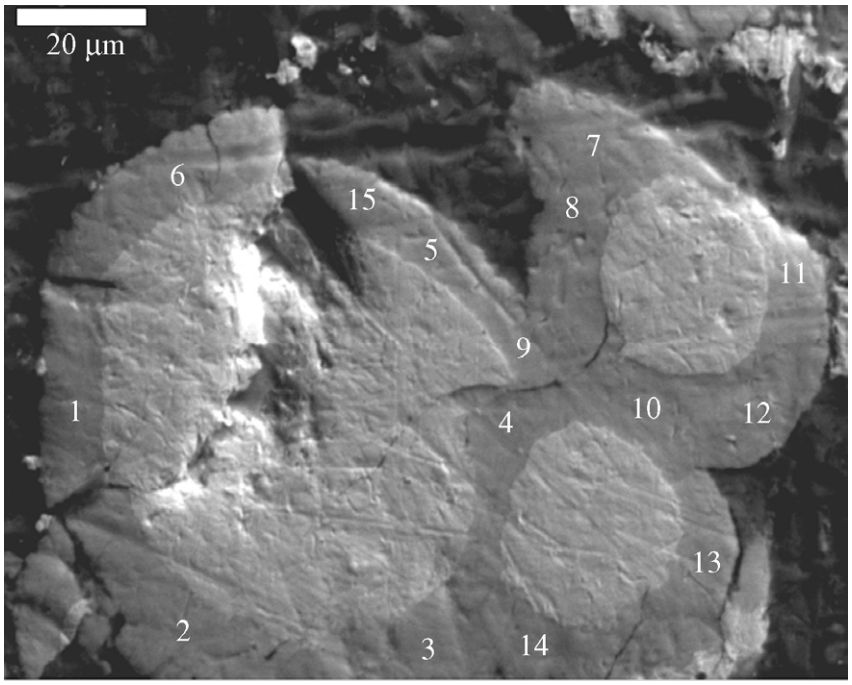

Figure 21. Locations on a secondary electron image showing where point-to-point analysis was performed to determine the composition of the interaction layer in sample R3R030B.

Table 4. Results of point-to-point EDS composition analysis, in at%, that was conducted at the locations in R3R030B, as shown in Figure 22.

Point	Al	Mo	U
1	82.3	2.6	15.1
2	81.6	2.7	15.8
3	83.6	1.7	14.8
4	81.7	2.9	15.5
5	83.6	2.1	14.2
6	81.7	3.4	15.0
7	83.6	1.8	14.6
8	82.2	2.1	15.7
9	82.6	2.3	15.2
10	81.9	3.3	14.8
11	83.2	1.6	15.2
12	83.3	2.5	14.3
13	80.6	3.7	15.8
14	83.2	2.1	14.7
15	80.9	2.8	16.3

4.2.3 R5R020

An SEM image of a longitudinal cross section of the R5R020 sample is presented in Figure 22. A large fraction of the middle portion of the sample is missing. This suggests that the punching passed through a region of the fuel plate where large porous regions were present (see Figure 10d), which allowed for sample loss during the punching process and subsequent sample preparation. The majority of the fuel material was present at each end of the punching. Secondary electron images centered around a large fuel particle found in R5R020 are shown in Figure 23. This particle is approximately 100 microns in diameter, making it one of the largest particles in the R5R020 fuel plate, based on Table 1. The interaction zone that is present around all the particles in this image appears to be uniform and is approximately 10 μm thick.

Possible porosity was identified within some of the fuel particles. Figure 24 shows locations in one of the particles where porosity, which was created during irradiation, was not smeared away during polishing. Also shown is an image of the interaction product, which does not appear to have any porosity.

WDS x-ray mapping was employed to determine the partitioning behavior of U, Mo, Al, and Si in sample R5R020. Figures 25 and 26 show x-ray maps for U, Mo, Al, and Si. The overall partitioning behavior for these constituents is analogous to what was observed for sample R3R030B, namely, that U and Mo are observed in the fuel alloy and interaction layer, Al is observed in the matrix and the interaction layer, and Si is observed in the precipitates in the matrix alloy and in some particles found in the U-7Mo alloy. Within the interaction layer, no composition gradients could be detected for U, Mo, or Al, indicative of a phase mixture as opposed to a single phase.

Point-to-point EDS analysis was performed on sample R5R020 to determine the interaction layer composition. The locations where these analyses were performed are shown in Figure 27. The composition analysis results are presented in Table 5. The minimum atomic percent values for Al, Mo, and U were 80.6, 1.6, and 14.3, respectively. The maximum atomic percent values Al, Mo, and U were 83.6, 3.6, and 16.3, respectively. The mean atomic percent values for Al, Mo, and U were 82.4, 2.5, and 15.1, respectively. The standard deviations were 1.0, 0.6, and 0.6 for Al, Mo, and U atomic percent values, respectively. The interaction layer composition values are in excellent agreement with what was observed for the R3R030B sample and also suggest the formation of a phase similar to a $(U,Mo)_{0.9}Al_{4.4}$ phase.

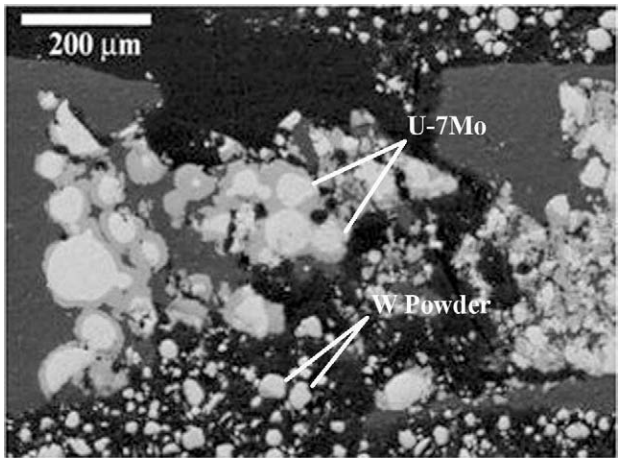

Figure 22. Backscattered electron image of a longitudinal cross section of the punching taken from sample R5R020. The bright contrast phases are either U-7Mo particles or W powder that was added to provide shielding. The medium contrast phase is interaction layer surrounded by dark contrast Al-0.2Si matrix.

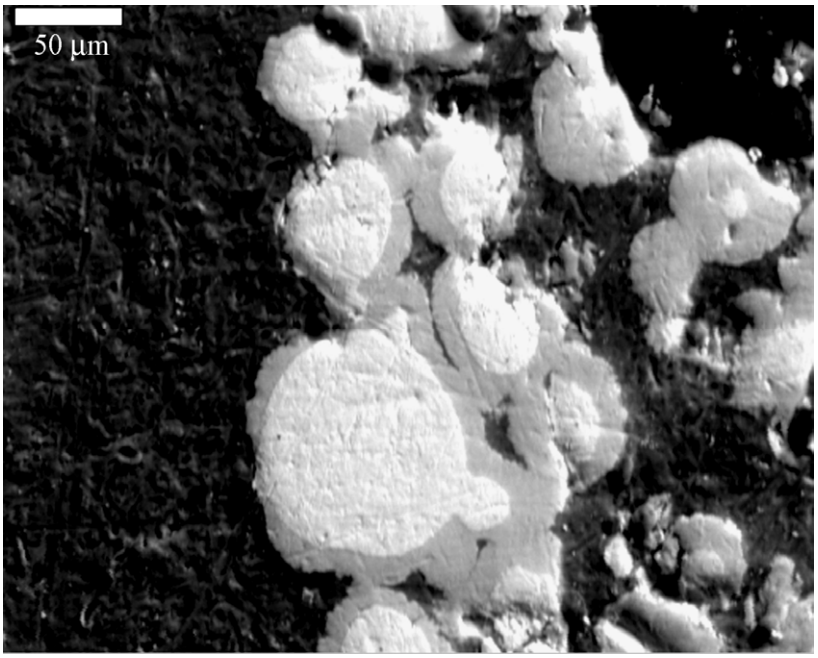

(a)

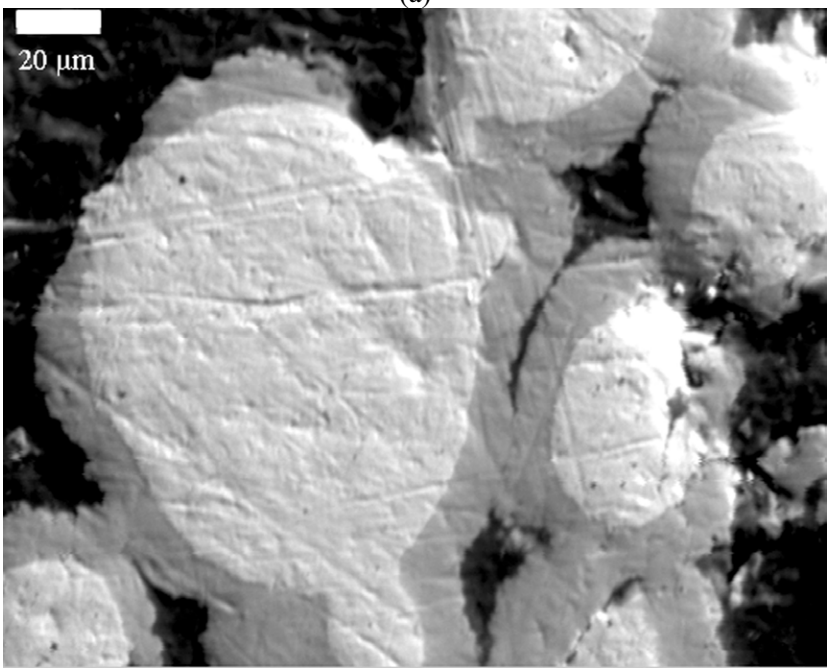

(b)

Figure 23. Low (a) and high (b) magnification secondary electron images of fuel particles observed in sample R5R020.

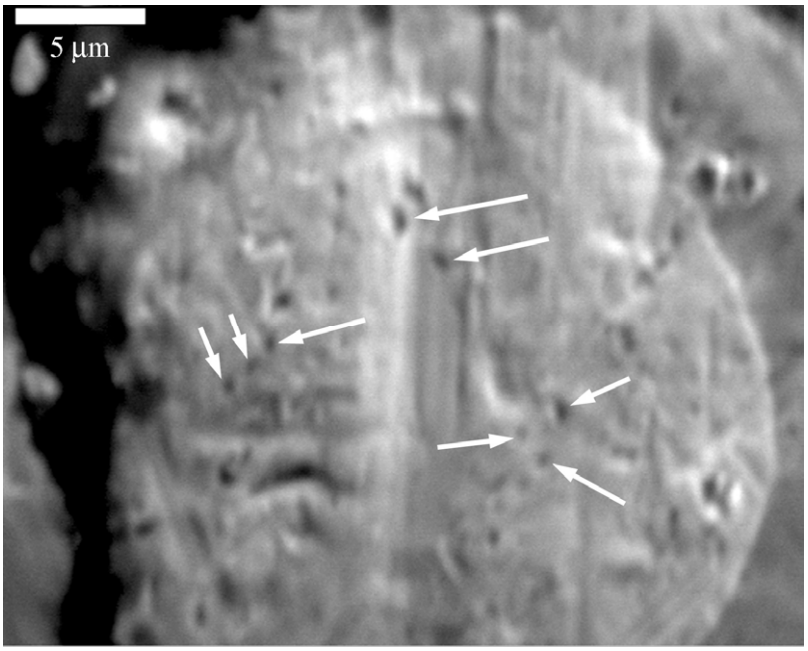

(a)

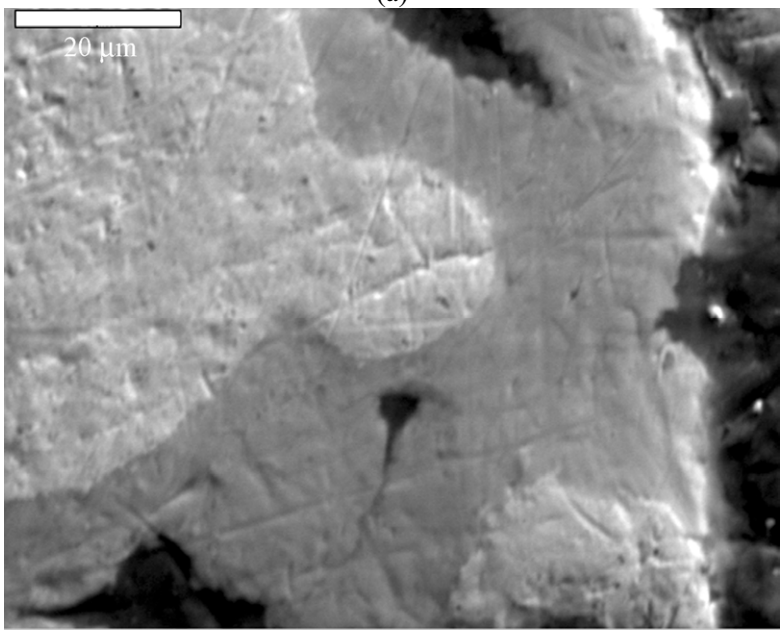

(b)

Figure 24. Secondary electron images of (a) a fuel particle and (b) interaction layer observed in sample R5R020. Arrows indicate locations where porosity may be present in the fuel microstructure.

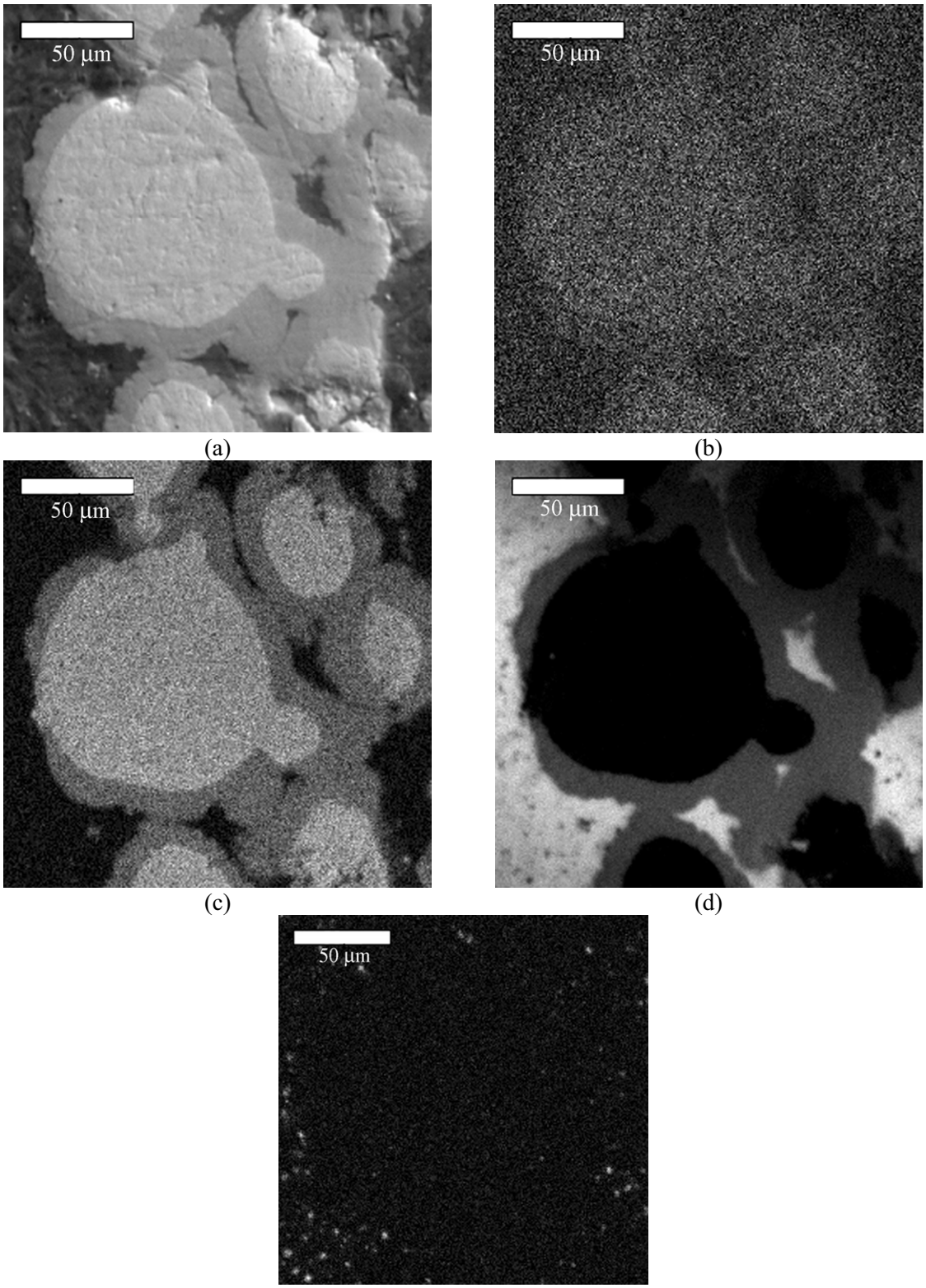

Figure 25. Secondary electron image and x-ray maps for (b) Mo, (c) U, (d) Al, and (e) Si taken for sample R5R020.

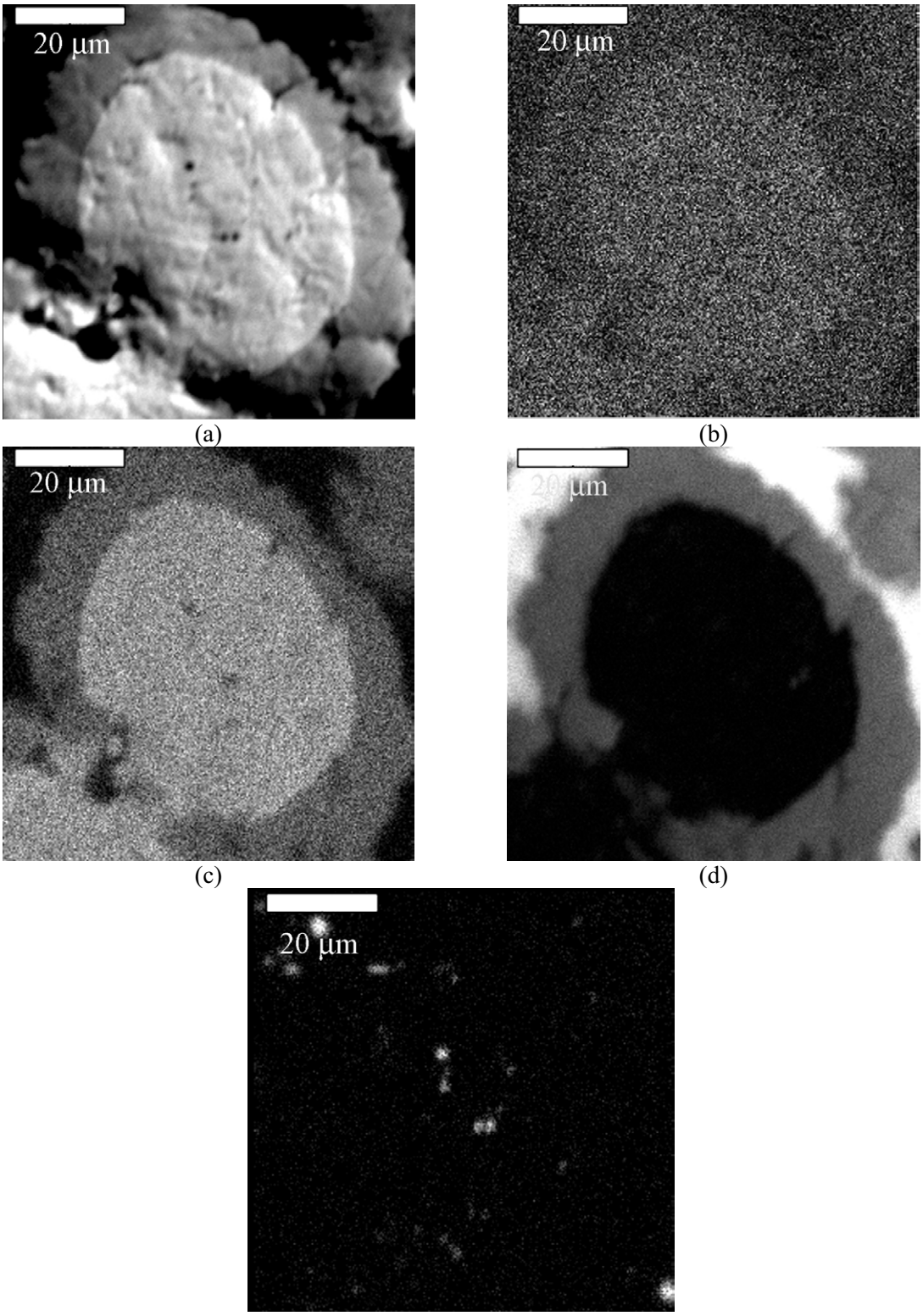

Figure 26. Secondary electron image and x-ray maps for (b) Mo, (c) U, (d) Al, and (e) Si taken for sample R5R020.

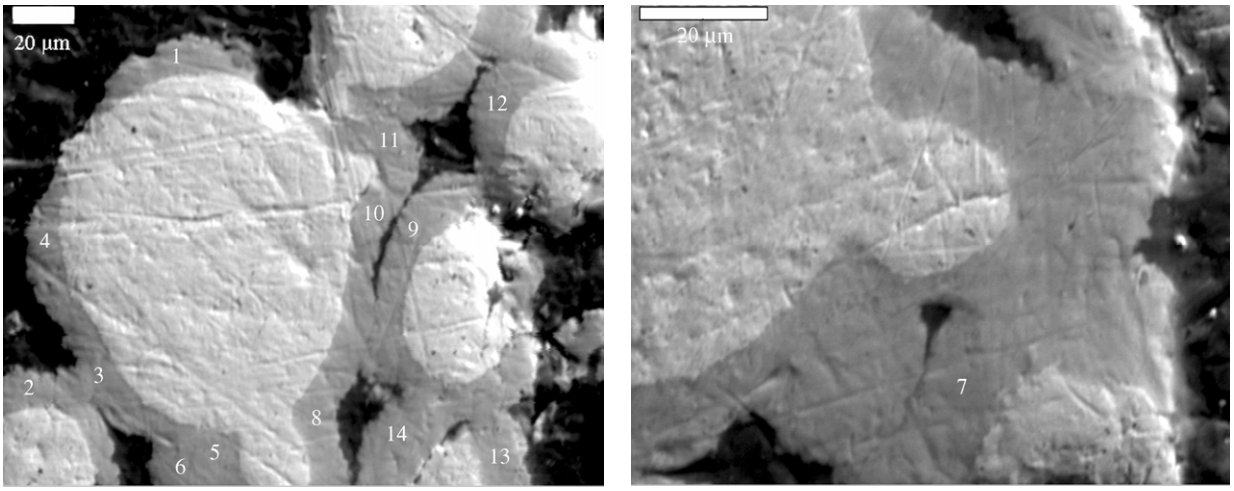

(a) (b)

Figure 27. Secondary electron images showing where point-to-point EDS analysis was conducted for sample R5R020 to determine the composition of the interaction layer.

Table 5. Results of point-to-point EDS composition analysis in at%, that was conducted at the locations in R5R020 shown in Figure 16.

Point	Al	Mo	U
1	82.7	3.7	13.5
2	84.8	3.4	11.8
3	81.6	2.7	15.7
4	81.1	3.3	15.6
5	82.5	1.8	15.7
6	81.2	3.1	15.7
7	83.6	2.7	13.7
8	84.9	2.1	13.0
9	83.5	1.4	15.1
10	83.6	2.6	13.8
11	84.3	2.6	13.2
12	83.9	2.9	13.2
13	80.1	4.6	15.3
14	85.4	0.3	14.2

5. DISCUSSION

Based on the results of the microstructural characterization that was performed on the irradiated fuel plates R3R030, R3R040, R3R050, and R5R020, there is a correlation with the partitioning behavior of Si during irradiation and the width of the interaction layers that are observed after irradiation. The thinnest interaction layers are enriched in Si, and the areas of the fuel plates where large areas of porosity can be observed correlate to areas where thicker, non-Si-containing interaction layers can be observed. These large layers are similar to what has been observed in irradiated U-Mo dispersion fuel plates that have only pure Al as the matrix.[3] As a result of these observations, it can be suggested that Si additions to the matrix of dispersion fuels will affect not only the kinetics of U-Mo/matrix interactions but also the types of phases that will form in these interaction layers. In irradiated U-Mo/Al matrix fuels, the development of very-Al-enriched phases have been correlated with poor fuel-plate performance at high burnups,[17] and the current results suggest that by adding Si, different, more stable, phases may be forming, and none of these phases are as enriched in Al as was the case for the U-Mo/Al matrix dispersion fuels.

5.1 Comparison to the literature

To develop better understanding of how adding Si may affect the microstructural development of the fuel plates during irradiation, it is beneficial to make comparisons with available irradiation performance data that is available in the literature. Table 6 lists details about reactor experiments that have been conducted using U-Mo dispersion fuels where information is given about interaction layer development. The IRIS-1 experiment tested a dispersion fuel of U-7.6 wt% Mo and Al in the OSIRIS reactor.[17,18] The U-Mo fuel was in the form of ground powder. To perform SEM and electron probe microanalysis (EPMA) analysis of the IRIS-1 fuel, three 15.4-mm-diameter punchings were used. All the samples displayed identical microstructures. Also listed in Table 6 are details about the interaction layer composition for the IRIS-2[19] and FUTURE[20,21] experiments. Like the IRIS-1 experiment, ground powder was employed in the IRIS-2 experiment. Conversely, the FUTURE experiment used atomized powder less than 125 μm in diameter. For the FUTURE experiment, exact compositions of the interaction layer have been reported. A phase with a composition of 15U-3Mo-82Al was observed, which agrees very well with the phase composition for the thick layers observed in the current study for both R3R030 and R5R020. For IRIS-2, changes in interaction product composition were observed as a function of moving from the “pillowing area” area of the plate (Al/[U+Mo] ratio of 4.5) to the edge of the meat (Al/[U+Mo] ratio of 6). This change in composition was also correlated to the temperature in the fuel plate. The ratio of 6 was at the coldest plate region and 4.5 at the hottest. For the lower temperature IRIS-1 test, a ratio of up to 8 was reported, and for the FUTURE test, which was at a higher temperature, the ratio was reportedly 3 to 4. Taking into account the errors involved in performing the compositional analysis, the results for the R3R030 and R5R020 samples show good agreement with those for the IRIS-2 and FUTURE experiments. An Al/(U+Mo) ratio near 4 has been measured in the interaction layer for the various plates. However, the Al/(U+Mo) ratio of 6 that was reportedly found in some interaction layers at the cold side of IRIS-2 was never observed for interaction layers in R3R030 or R5R020, even though R3R030 had a peak cladding temperature that was colder than that reported for IRIS-2. For the FUTURE test, an Al(U+Mo) ratio of 7 was observed in the area of the plate where there were large pores, whereas the R5R020 fuel plate exhibited an Al/(U+Mo) ratio of 4.7 for the interaction layers near areas of large porosity. The IRIS-3 experiment tested a U-7.3 wt% Mo dispersion fuel with Al-2.1 wt% Si alloy as the matrix.[22,23] A jagged interaction layer was observed to form around the U-Mo particles, and x-ray maps showed that layers enriched in Si were present at some locations. Overall, the thinnest layers corresponded to areas with the highest concentrations of Si, and it was suggested that Si precipitates were present near the thinnest layers. The most commonly observed phase had an (Al+Si)/(U+Mo) ratio near 4, and this phase was not observed to be highly enriched in Si. Around 2.0 wt% (~5 at%), Si was the highest concentration reported in this interaction layer. Comparisons between R3R030, R5R020, and IRIS-3 will

be discussed later in this paper. For IRIS-TUM, no comparisons can be made to the interaction layer compositions observed in other experiments because no Al/(U+Mo) ratio has been reported.

Table 6. Comparison of the calculated values for peak temperature, fission density, fission rate, peak heat flux, and interaction zone thickness for plates R3R030 and R5R020 with those reported for the irradiated dispersion plates IRIS-1,[17] IRIS-2,[17] IRIS-3,[17,21] IRIS-TUM,[17,22] and FUTURE.[17,20]

Experiment (Sample)	Matrix	Calculated Peak Cladding Temperature (°C)	Fission Density (Plate Ave.) (10^{21} fcm^{-3})	Ave. Fiss. Rate (Burnup) (10^{14} fcm^{-3}s^{-1})	Peak Heat Flux for entire plate (W/cm^2)	Interaction Zone Thickness (μm)	Al/(U+Mo) ratio
IRIS-1	Al	69	3.2	1.5	124	4 to 6	6[a] to 8[b]
IRIS-2	Al	93	2.2	4.4	238	7 to 10	4.6 to 5.8
IRIS-3	Al-2Si	83	3.4	3.0	196	1 to 6	~4[c]
IRIS-TUM	Al	103	4.2	3.6	~250	~5	NR
IRIS-TUM	Al-2Si	103	4.2	3.6	~250	~5	NR
FUTURE	Al	130	1.41	6.3	353	4[d] to 11[e]	3.3 to 4.7
R3R030	4043 Al	81	2.80	2.3	101.5	10[f] ;1.5[g]	4.7[h]
R5R020	Al-0.2Si	108	2.83	3.5	130.5	10	4.7

a. (for BU=61%)
b. (for BU=67.5%)
c. Si is combined with Al to get this ratio
d. for low heat flux region of plate
e. for high heat flux region of plate
f. thickness based on SEM analysis of one punching
g. thickness based on optical metallography analysis of one transverse cross section of the plate taken at the midplane and SEM analysis of one punching
h. Measurement for 10-μm-thick layer with negligible Si; Si-rich layer too thin to reliably determine composition.
NR Not Reported.

The data discussed above is for plate-type fuels, but observations from irradiated pin-type fuels that were run as part of the KOMO-2[24] and KOMO-3[25] experiments can also be compared. For KOMO-2 in the fuel regions of the pin-type fuels that consisted of <150-μm- diameter U-7Mo particles in Al that reached 50%, 62%, and 68% burnups, compositional analysis was performed on the interaction layers. In general, there was very little change in composition throughout the thickness of the interaction layers, and for the lower temperature regions of the fuel, a (U,Mo)Al_4 phase was observed, and in the higher temperature regions, a (U,Mo)Al_3 phase was observed. The (U,Mo)Al_4 phase had an approximate composition of 15U-3Mo-82Al. The BOL temperatures that were calculated for the 50%, 62%, and 68% burnup samples were 134.2°C, 167.3°C, and 188.9°C, respectively. The peak fuel temperatures for these samples were calculated to be 143°C, 280°C, and 334°C, respectively. All three of the samples that saw different burnups formed a (U,Mo)Al_4 phase in the center and/or outer periphery of the fuel.

For the KOMO-3 experiment, the performance of fuel plates with 210 to 300-μm-diameter U-7Mo fuel particles and Al or Al-2.0 wt% Si alloy matrices were compared. The fuel pin with Al matrix was irradiated to 63.2% burnup at the fuel meat center and had a maximum BOL temperature of 170°C, while the Al-2.0 wt% Si matrix fuel element was irradiated to 64.87% burnup at the fuel meat center and had a maximum BOL temperature of 174°C. It was observed that the composition of the interaction layers that formed at the interface between the U-7Mo fuel particles and the matrix were very similar regardless whether the matrix was Al or Al-2.0 wt% Si. A (U,Mo)Al_3-type phase was observed for the highest temperature regions of the fuel elements, and a (U,Mo)Al_4-type phase was observed to develop in the colder regions. For the fuel element with Al-2.0 wt% Si matrix, up to 11.0 at% Si was measured in the (U,Mo)(Al,Si)$_3$ phase, and up to 4.0 at% Si was observed in the (U,Mo)(Al,Si)$_4$-type phase. Overall, the

interaction layer thickness was decreased for the fuel with a Si-containing matrix (~40 μm) compared to the one that had pure Al (~70 μm).

5.2 Development and behavior of Si-rich layers

There is general agreement in the literature that adding Si to the matrix improves U-Mo dispersion fuel plate performance. In general, the amount of interaction is reduced, and more stable fuel behavior is observed. In other words, the gross porosity that can link up and cause fuel failure is not observed. This agrees with the observations made as part of the current investigation. One difference between the samples discussed in this paper and those used in the experiments described in Table 6 is that pre-existing Si-rich layers were present around the fuel particles for the R3R030, R3R040, R3R050, and R5R020 fuel plates and reportedly are not present in the as-fabricated, Si-containing matrix fuel plates irradiated in the IRIS-3 and IRIS-TUM experiments.[26] For the KOMO-3 pin-type fuel element test, there was also no fuel/matrix interaction after pin fabrication.[27] The rolling temperatures used to fabricate the IRIS-3 and IRIS-TUM fuel plates were lower than those used to fabricate the fuel plates discussed in this paper. This is because the AlFeNi (IRIS-TUM) and AG3NE (IRIS-3) claddings that were employed for the other fuel plates were softer alloys than the 6061 Al alloy cladding used for the fuel plates discussed in this paper and could be rolled at lower temperatures (in the mid-400°C range compared to 500°C). Rolling at temperatures lower than 500°C has a significant impact on the amount of interaction that will occur between U-7Mo and Al alloys. The overall kinetics of the interaction are reduced because diffusion rates are lower at lower temperatures, and, perhaps more significantly, decomposition of the γ-phase U-7Mo alloy has been found to start within times as short as 10 minutes at 500°C,[12] which increases the rate of interaction for a U-7Mo alloy with Al alloys when compared to pure γ-phase alloys.[5] The nose of the Time Temperature Transformation (TTT) curve for γ-phase U-Mo alloys to begin transforming to α-U + γ' (U_2Mo) is near 500°C.[28] Therefore, temperatures in the mid-400°C range are below the nose of the TTT curve, and, as a result, it takes hours before γ-phase U-7Mo starts to decompose and increase interaction rates. So, if the U-7Mo alloy remains γ-phase during fabrication, then the interaction rates with Al alloys are much more sluggish.[5]

When dispersion fuels do not form interaction layers during fabrication, then any layers that are present after irradiation are formed due to radiation enhanced diffusion (RED). The temperatures that fuel plates are exposed to during irradiation are low enough (typically around 100°C and, at most, 200°C) that any thermal diffusion component should be negligible, and, therefore, any interaction that takes place appears to be due to RED. Si present in interaction layers created by RED probably comes from the Si that is present as precipitates in the matrix alloy in the recoil zones around the fuel particles (~10 μm). The fission fragments and localized heating in these regions dissolves the Si precipitates, and the Si diffuses to the U-7Mo/matrix interface to help form phases. On the other hand, for the fuels where Si-rich phases are created during fabrication, Si diffuses to the interface due to thermal diffusion at the near 500°C fabrication temperatures and is present as phases in the formed layers. This Si comes from locations in the matrix that are further away than the thickness of a recoil zone. As a result, a Si-rich layer is already present when the irradiation process takes place. Based on composition, these Si-rich layers have an (Al+Si)/(U+Mo) ratio near 2, which is different than the more typical ratio of 3 to 4 that is measured for interaction phases after irradiation. Additional Si will diffuse to the U-7Mo/matrix interface during irradiation and will come from the matrix within the recoil zones.

For the initial Si-rich phases to remain stable during irradiation, it appears that a certain amount of Si has to diffuse to the interaction layer during irradiation, or else the Si-rich layer will become unstable, and the diffusion processes that are typical for the U-Mo-Al system take over. When this happens, the Si that was contained in the interaction layer precipitates out as an Si-rich phase in the Al alloy matrix near the interaction layer. Therefore, there needs to be enough Si added to the matrix to keep the initial Si-rich layers stable. Based on the characterization of the Al-0.2 wt% Si dispersion fuel, and the fact that the

layers were relatively thick and no Si-rich layers were observed in the irradiated sample, it seems that 0.2 wt% Si is not enough of an addition to the Al matrix to keep any formed Si-rich layers stable during irradiation. Whereas, for the fuel plate with 4043 Al alloy matrix, thin, Si-rich layers could be found after irradiation of a fuel plate to high-fission densities. On the other hand, analysis of another sample taken from the fuel plate indicated the presence of thicker Si-deficient layers, which suggested that the 4.81 wt% Si present in the alloy was enough to keep Si-rich layers stable under most irradiation conditions, but not the most aggressive conditions, where the second SEM sample was taken. Therefore, interaction layers only begin to break down in areas of a fuel plate exposed to very high fission densities that cause porous areas to develop. However, the fission densities where breakdown occurs seem to be well beyond where a typical research reactor fuel plate would be taken. Yet, it is still of value to obtain performance data up to these high fission-density levels to determine the overall margins of the fuel.

A full understanding of the performance of as-irradiated U-Mo dispersion fuels with matrices that contain Si seems to require that more samples be characterized using an SEM or electron microprobe, which will enable a better understanding of how making additions to the matrix or fuel will affect the formation of interaction layers. Samples with varying Si additions to the matrix that have been irradiated under a variety of conditions should be analyzed in an attempt to determine the mechanisms by which the presence of Si in the matrix influences interactions with the fuel. This work should also include the use of x-ray diffraction so that the crystal structures of the developed phases can be determined. It has been shown that when U-Mo dispersion fuels with Al as the matrix are irradiated at relatively low temperatures, the interaction layers that form are amorphous,[29] and amorphous layers may display different performance characteristics relative to phases that are crystalline. As a result, it is of interest to determine if interaction layers that form in U-Mo dispersion fuels with Al alloys that contain Si as the matrix are also amorphous.

6. CONCLUSIONS

U-Mo dispersion fuel plates with matrices that contained Si were irradiated in the Advanced Test Reactor as part of the RERTR-6 and RERTR-7 experiments. Based on destructive examination of the plates performed using optical metallography and SEM/EDS/WDS analyses, the following conclusions can be drawn:

1. Under the reactor conditions of both the RERTR-6 and RERTR-7 experiments, U-7Mo dispersion fuels with 4043 Al alloy (4.81 wt% Si) matrix exhibit overall thinner interaction layers between the U-7Mo fuel particles and the matrix, compared to irradiated U-Mo dispersion fuels with relatively pure Al as the matrix. Porous areas are not observed in most areas of the irradiated fuel plates and only seem to develop in the areas of the fuel plates that are exposed to the most aggressive reactor conditions (~100% LEU burnup), which are beyond what a typical research reactor fuel would see. Conversely, not much difference is seen between the microstructural development of a dispersion fuel with Al-0.2 wt% Si matrix and what is seen for dispersion fuels with pure Al as the matrix. Therefore, it appears that there is a minimum Si addition to the matrix to achieve the improved fuel performance that is necessary for taking U-Mo dispersion fuels to the more aggressive reactor conditions.
2. For as-fabricated dispersion fuel plates with pre-existing, Si-rich interaction layers, there seems to be a difference in fuel behavior during irradiation relative to fuel plates that do not have these layers after fabrication. When fuel plates contain as-fabricated, Si-rich interaction layers, these layers do not increase significantly in thickness during irradiation, except under very aggressive reactor conditions. On the other hand, fuel plates with no as-fabricated interaction layers seem to develop micron-thick layers during irradiation that do not appear to be as Si-rich. In terms of interaction layer composition, no Al-rich layers (with an Al/[U+Mo] ratio of 7 or 8), which can be linked to poor fuel performance in U-Mo/Al matrix fuels, have been observed to form in U-Mo dispersion fuels with Al matrices that contain Si.

7. REFERENCES

1. J. L. Snelgrove, et al., Nucl. Engr. and Design 178 (1997) 119.
2. D. M. Wachs, et al., Proc. of Global 2007: Advanced Nuclear Fuel Cycles and Systems Conference, Boise, Idaho, 2007.
3. A. Leenaers, et al., J. Nucl. Mater. 335 (2004) 39.
4. Y. S. Kim, et al., Proc. of the 25th International Meeting on Reduced Enrichment for Research Reactors, Boston, MA, 2005.
5. D. D. Keiser, Jr., Defect and Diffusion Forum, 266 (2007) 131.
6. E. Perez, et al., Defect and Diffusion Forum, 266 (2007) 149.
7. H. J. Ryu, et al., J. Phase Equil. And Dif. 27 (6) (2006) 651.
8. A. Leenaers, et al., J. Nucl. Mater. 327 (2004) 121.
9. K. H. Kim, J. Nucl. Mater. 245 (1997) 179.
10. C. R. Clark, et al., Proc. of the 27th International Meeting on Reduced Enrichment for Research and Test Reactors, Prague, Czech Republic, 2007.
11. T. C. Wiencek, Argonne National Laboratory Report No. ANL/RERTR/TM-15, 1995.
12. J. M. Park, et al., Proc. of the 26th International Meeting on Reduced Enrichment for Research and Test Reactors, Cape Town, South Africa, 2006.
13. L. S. Castleman, J. Nucl. Mater. 3 (1961) 1.
14. D. E. Janney, et al., Hot Laboratories and Remote Handling Plenary Meeting, Bucharest, Romania, September 20-21, 2007.
15. D. Olander, J. Nucl. Mater. 372 (2008) 94.
16. T. B. Massalski, ed. Binary Alloy Phase Diagrams, 2nd Ed. (American Society for Metals, Metals Park, OH, 1990).
17. F. Huet, et al., Proc. of the 23rd International Meeting on Reduced Enrichment for Research and Test Reactors, Chicago, Illinois, 2003.
18. S. Dubois, et al., Eleventh International Topical Meeting on RRFM, Lyon, France, 2007.
19. F. Huet, et al., Ninth International Topical Meeting on RRFM, Budapest, Hungary, 2005.
20. A. Leenaers, et al., Eighth International Topical Meeting on RRFM, Munich, Germany, 2004.
21. A. Leenaers, et al., J. Nucl. Mater. 335 (2004) 39-47.
22. A. Leenaers, et al., Twelfth International Topical Meeting on RRFM, Hamburg, Germany, 2008.
23 M. Ripert, et al., Twelfth International Topical Meeting on RRFM, Hamburg, Germany, 2008.
24. J. M. Park, et al., Proc. of the 24th International Meeting on Reduced Enrichment for Research and Test Reactors, Vienna, Austria, 2004.
25. J. M. Park, et al., Twelfth International Topical Meeting on RRFM, Hamburg, Germany, 2008.
26. C. Jarousse, AREVA-CERCA, Hamburg, Germany, March 4, 2008, personal communication.

27. C. K. Kim, et al., Proc. of the 25th International Meeting on Reduced Enrichment for Research and Test Reactors, Boston, MA, 2005.

28. G. L. Hofman and L. C. Walters, *Materials Science and Technology: A Comprehensive Treatment, Vol. 10*. Ed. R. W. Cahn, P. Haasen, and E. J. Kramer. New York: VCH Publishers Inc., 1994. p. 13.

29. S. Van den Berghe, et al., Proc. of the 27th International Meeting on Reduced Enrichment for Research and Test Reactors, Prague, Czech Republic, 2007.